Charles University
Faculty of Mathematics and Physics

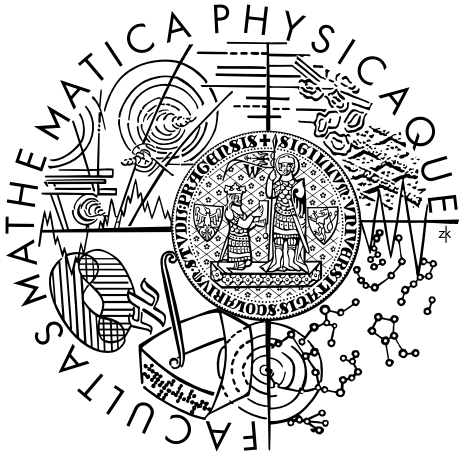

Martin Žofka

Selected exact solutions of Einstein equations and their properties

HABILITATION THESIS
Prague 2020

Contents

Introduction **3**

1 Gravito-magnetic fields **5**
1.1 Homogeneous magnetic field 6
1.2 Special non-homogeneous magnetic field 10
1.3 General solution 14

2 Spacetime crystals **17**
2.1 Like charges 17
2.2 Unlike charges 21
2.3 Dimensional reduction 23

3 Spacetime locomotion **25**
3.1 Swimming dumbbells? 25
3.2 Discrete spring 29

4 Higher dimensions **33**

5 Cylinders **35**

Bibliography **37**

6 Selected original papers **45**

Introduction

Ever since the advent of general relativity, exact solutions have played a crucial role in the quest to understand the deeper workings of the spacetime physics. Indeed, how do we know how to read a given numerical solution of Einstein equations? How do we know what boundary conditions to impose at infinity or on an initial Cauchy hypersurface? How to infer the physical mass and angular momentum of a galactic black hole from observations of stars orbiting around it? All these questions beg us to build up our intuition about exact solutions that approximate real-world situations in a manner characterized by a set of parameters with a clear meaning from the point of view of physics. It is in fact precisely these parameters that we want to infer from our observations of phenomena taking place in the vicinity of black holes and other general-relativistic objects in the Universe.

In this thesis I aim to review my recent and ongoing research into several topics concerning two very different classes of solutions to Einstein–Maxwell equations and motion of toy-models of extended bodies in curved spacetimes. I also briefly cover my work on higher-dimensional extensions of Einstein gravity and my general field of interest—cylindrically symmetric solutions. Throughout the text, I use the standard geometrized units, setting $c = G = 1$. In Chapter 1, I present a generalization of the well-known Bonnor–Melvin cylindrically symmetric solution, which involves a magnetic field aligned with the axis of symmetry. The gravitational field is due solely to the magnetic field that, in turn, feels the gravitational tug so the two fields are a fully self-consistent solution of Einstein–Maxwell equations. The solution has one drawback as compared to the classical, purely Maxwellian solution—it lacks homogeneity. I mend this glitch by generalizing the solution to include the cosmological constant countering the gravitational pull. Furthermore, I find an even more general solution, which is again no longer homogeneous but includes the previous two as special cases, and I suggest a way forward in generalizing even this spacetime. Chapter 2 discusses what happens if we combine multiple black-hole solutions together. Einstein equations are generally non linear and thus we cannot apply the superposition principle but there is a special family of solutions—the Majumdar–Papapetrou solutions of Einstein–Maxwell equations—where the field equations all collapse to yield a single flat-space Laplace's equation, a linear equation describing both their gravitational and electromagnetic fields. This only applies to a very special class of black holes bearing electric charges equal to their masses. Curiously, the resulting static spacetime is kept in balance by precisely the same principle as in classical Newtonian physics where the gravitational attraction is exactly canceled by the electrostatic repulsion. I now pose the question: what happens if we keep adding the black holes ad infinitum? To be able to formulate the answer I assume the black holes form a crystal-like one-dimensional lattice. I present several possible approaches to the problem and discuss their merits and drawbacks. In Chapter 3, I deal with the problem of motion of non-point-like objects in general relativity. This topic is customarily dealt with through the so-called Dixon formalism, which applies to general bodies complying with the law of conservation of stress-energy tensor. However, I concentrate specifically on very simple situations where the test body consists of several interacting mass points and so it is much simpler to work starting directly from the first principles. I am interested in the motion of the test body as compared to the motion of simple point particles with analogous initial conditions. This problem relates to the so-called spacetime swimming and swinging effects whereby objects can modify their trajectories by going through cyclic deformations. In fact, the same occurs in Newtonian physics and it has even been tested in-orbit with satellites releasing masses attached to them via tethers to

stabilize their rotation and adjust its direction. I study two basic toy models of bodies falling freely in the gravitational field of the Schwarzschild black hole to see whether the previously reported swimming effect indeed occurs. I conclude with two brief sections on two more areas of interest to me: Chapter 4, which deals with generalizations of spacetimes for a number of dimensions higher than 4 and discusses some special classes of these solutions, and the final Chapter 5, which describes my work on certain families of cylindrically symmetric solutions of Einstein equations, including both vacuum fields and spacetimes due to matter.

Most of the work presented in the thesis has been published and I include some of the corresponding papers as attachments hereto. I have attempted to present here a broader perspective of the topics covered by the papers. I hereby acknowledge and appreciate the contribution, support, and company of my students—Jiří Ryzner, Jiří Veselý, and Vítek Veselý—who have been instrumental in helping my find a way forward when tackling the problems mentioned above and who have coauthored many of my papers. It is also thanks to my colleagues, and particularly Tomáš Ledvinka, that I have had enough courage to work on the mathematics and physics included here at times when the equations just seemed not to work out (and when I was brave enough to ask for help).

And finally, but first of all—thank you, Pop!

1 Gravito-magnetic fields

In this chapter, we wish to investigate self-consistent solutions of Einstein–Maxwell equations describing magnetic fields that gravitate and are in balance with their own gravitational field. Let us begin with a discussion of the classical homogeneous magnetic field without considering the gravitational field it generates. Put differently, we want the Minkowski spacetime with a homogeneous test magnetic field. This is a simple enough task and—using cylindrical coordinates (t, r, z, φ) since the field is obviously also cylindrically symmetric—the field is described by a Maxwell tensor of the form

$$F_{r\varphi} = Hr, \tag{1.1}$$

while all the other components vanish and the non-vanishing Maxwell invariant reads $F_{\mu\nu}F^{\mu\nu} = 2H^2$ where H is the strength of the constant magnetic field, which is directed along the z-axis and permeates the entire space.

The situation changes completely if we include the back-reaction of the field on the spacetime. To do this, we need to consider not only Maxwell equations but also Einstein equations. The solutions of the full set of Einstein–Maxwell equations include an interesting spacetime discovered in 1954 by Bonnor [1], rediscovered in 1964 by Melvin [2], and describing a static, cylindrically symmetric magnetic field held against gravitational collapse by its own pressure due to the Maxwell stress tensor—this is thus the so-called geon [3, 4, 5]. The corresponding line element written in cylindrical coordinates is given as

$$g_{\mu\nu} = \alpha^{-2}(-\mathrm{d}t^2 + \mathrm{d}z^2) + \alpha^{-5}\mathrm{d}r^2 + \alpha r^2 \mathrm{d}\varphi^2, \tag{1.2}$$

where

$$\alpha = 1 - K^2 r^2, \tag{1.3}$$

and $r < 1/K$ (see also [6], p. 317). Let us mention some of the properties of the solution here. The surface located at $r = 1/K$ at an infinite proper distance from the axis cannot be reached in a finite time even by photons and all timelike geodesics have their turning points closer to the axis. The circumference $\mathcal{C}$ of hoops $t, z, r = \text{const.}$ reaches its maximum value of

$$\mathcal{C}_{\max} = \pi/K \tag{1.4}$$

at $r = 1/K\sqrt{2}$ or $\alpha = 1/2$ and then decreases to zero again (see Figure 1.1). The spacetime thus has two axes separated by an infinite radial distance. The solution is regular on the symmetry axis as it ought to be to avoid any singularity that would influence the gravitational and magnetic fields—but is this a homogeneous field? We must answer in the negative since the Maxwell field reads

$$F_{r\varphi} = 2Kr, \tag{1.5}$$

with the corresponding invariant

$$F_{\mu\nu}F^{\mu\nu} = 8K^2\alpha^4. \tag{1.6}$$

Therefore, the invariant decreases with increasing distance from the axis, resulting in a non-homogeneous field. This is a natural consequence of the fact that the energy of the magnetic field curves the spacetime. However, it only changes slowly near the axis representing thus a good approximation of the classical homogeneous field here. Since there are no singularities present in the spacetime and as the field equations for the magnetic field are vacuum Maxwell equations, the source of the electromagnetic field must reside at infinity. In our previous work

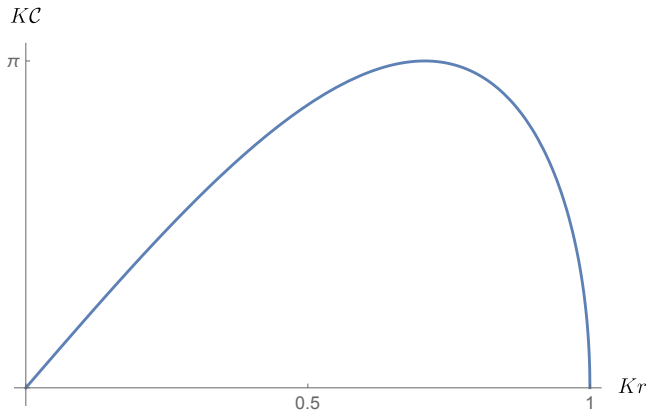

Figure 1.1: Circumference $\mathcal{C}$ of rings $t, z, r = \text{const.}$ in the Bonnor–Melvin universe. The peak is located at $r = 1/K\sqrt{2}$ or $\alpha = 1/2$. Vanishing circumference signifies the presence of an axis.

we constructed a shell source of the field in the form of an infinite cylinder enveloping the axis and consisting of streams of charged particles spiralling along its surface [7]. Inside the shell, there was the Bonnor–Melvin field in analogy with a classical infinite solenoid while the outside section of the spacetime was described by the Levi-Civita solution [8].

What then can one do to obtain a homogeneous solution with a Maxwell invariant constant throughout the spacetime? We need a counteracting force that would balance the total gravitational pull of the magnetic field contained in any cylinder aligned with the axis. In other words, we need an antigravitating agent. Luckily, such a means is readily at hand in the form of the cosmological constant Λ due to Einstein [9] who used it with exactly the same aim—to prevent a collapse of the universe. The currently observed value of the constant is positive [10], which plays nicely into our hands.

1.1 Homogeneous magnetic field

We are looking for a static, cylindrically symmetric solution of Einstein–Maxwell equations [6, 11] with the cosmological term corresponding to a positive (repulsive) cosmological constant enabling and upholding the now homogeneous magnetic field. To comply with the symmetry of the source, we shall assume the same symmetry for the gravitational field as well[1] and we shall keep the cylindrical coordinate system to write the metric as

$$ds^2 = -\exp A(r)\, dt^2 + dr^2 + \exp B(r)\, dz^2 + \exp C(r)\, d\varphi^2, \tag{1.7}$$

here $t, z \in \mathbb{R}, r \in \mathbb{R}^+, \varphi \in [0, 2\pi)$, and r denotes the proper radius. This is the general form of any metric with the required symmetries [13]. Thus far, we have reduced the problem to finding the 3 unknown functions of one variable—$A(r), B(r)$, and $C(r)$. We now proceed to

[1] In fact, the gravitational field and its source matter fields do not need to share the same symmetry [12]. For an example, see Chapter 2, where the source scalar field of an axially symmetric spacetime is not axially symmetric itself.

derive the Einstein tensor components combined with the cosmological term:

$$G_{tt}-\Lambda g_{tt} = \frac{1}{4}\mathrm{e}^{A}\left(2B''+(B')^2+2C''+(C')^2+C'B'+4\Lambda\right), \tag{1.8}$$

$$G_{rr}-\Lambda g_{rr} = -\frac{1}{4}A'B'-\frac{1}{4}A'C'-\frac{1}{4}B'C'-\Lambda, \tag{1.9}$$

$$G_{zz}-\Lambda g_{zz} = -\frac{1}{4}\mathrm{e}^{B}\left(2A''+(A')^2+2C''+(C')^2+A'C'+4\Lambda\right), \tag{1.10}$$

$$G_{\varphi\varphi}-\Lambda g_{\varphi\varphi} = -\frac{1}{4}\mathrm{e}^{C}\left(2A''+(A')^2+2B''+(B')^2+A'B'+4\Lambda\right), \tag{1.11}$$

with primes denoting derivative with respect to the radial coordinate. As the next step we require a purely magnetic field with field lines parallel to the axis of symmetry and arrive at a Maxwell tensor of the form

$$F_{r\varphi} = H(r). \tag{1.12}$$

This fixes the invariant of the magnetic field to

$$F_{\mu\nu}F^{\mu\nu} = 2H^2\mathrm{e}^{-C} =: 2f^2, \tag{1.13}$$

where we defined a new quantity, the function $f(r)$. This is a scalar value independent of the coordinate system and measurable by any observer. It is therefore precisely this quantity that we shall use to characterize the field. Comparing our expressions to the homogeneous test field in Minkowski—see relation 1.1 and below—we see that the analogy suggests $f = H$, with H the magnetic field strength. We can now write down the corresponding stress-energy tensor of the electromagnetic field

$$T_{tt} = \frac{1}{8\pi}\mathrm{e}^{A-C}H^2, \tag{1.14}$$

$$T_{rr} = \frac{1}{8\pi}\mathrm{e}^{-C}H^2, \tag{1.15}$$

$$T_{zz} = -\frac{1}{8\pi}\mathrm{e}^{B-C}H^2, \tag{1.16}$$

$$T_{\varphi\varphi} = \frac{1}{8\pi}H^2, \tag{1.17}$$

which forms the right-hand side of the final Einstein equations. After some algebra, we obtain

$$0 = 2(B''+C'')+(B')^2+(C')^2+B'C'+4\Lambda+4f^2, \tag{1.18}$$

$$0 = 2(A''+C'')+(A')^2+(C')^2+A'C'+4\Lambda+4f^2, \tag{1.19}$$

$$0 = 2(A''+B'')+(A')^2+(B')^2+A'B'+4\Lambda-4f^2, \tag{1.20}$$

$$0 = A'B'+A'C'+B'C'+4\Lambda-4f^2. \tag{1.21}$$

We see that, in fact, this is a set of three second-order ordinary differential equations plus an equation defining the value of the function f. The set is invariant with respect to interchanging the functions A and B, which is to be expected in view of the fact that the corresponding coordinates, t and z, appear symmetrically in the metric 1.7. This does not mean that every solution to these equations is symmetric in this respect but that it might make sense to look for such a solution and we shall return to this point in the following section. We now turn to

Maxwell equations $\sqrt{-g}F^{\mu\nu}{}_{;\nu} = (\sqrt{-g}F^{\mu\nu})_{,\nu} = 0$ to see whether they constrain the solution in any way but we conclude that these are identities apart from

$$\begin{aligned}\sqrt{-g}F^{\varphi\alpha}{}_{;\alpha} &= (\sqrt{-g}F^{\varphi r})_{,r} = (\mathrm{e}^{\frac{A+B-C}{2}}F_{\varphi r})_{,r} = \\ &= -(\mathrm{e}^{\frac{A+B-C}{2}}H)_{,r} = -(\mathrm{e}^{\frac{A+B}{2}}f)_{,r} = 0,\end{aligned} \tag{1.22}$$

which implies

$$\mathrm{e}^{\frac{A+B}{2}}f = const. \tag{1.23}$$

This, however, is a consequence of Einstein equations as well and thus contains no additional information that would help us solve the field equations.

Requiring now a homogeneous magnetic field with a constant invariant, $F_{\mu\nu}F^{\mu\nu}$, we use the definition 1.13 to translate this to

$$f = const. \tag{1.24}$$

This assumption simplifies our equations immensely—we immediately infer from (1.23) that $A + B = const.$ But (1.20)+(1.21) then imply

$$2(A+B)'' + ((A+B)')^2 + C'(A+B)' + 8(\Lambda - f^2) = 0 \tag{1.25}$$

and, therefore, finally

$$f^2 = \Lambda. \tag{1.26}$$

Notice that we necessarily have $\Lambda > 0$, as expected—the cosmological constant balances the gravitational self-attraction of the magnetic field, preventing its collapse. We still need to determine the metric coefficients: using (1.21), we find $A'B' = 0$ and combining this with $A' + B' = 0$ derived above, we have

$$A = const., B = const. \tag{1.27}$$

Next, we use the coordinate gauge freedom and rescale t and z to choose $A = 0$, $B = 0$, without loss of generality. We are left with a single Einstein equation

$$C'' + \frac{1}{2}C'^2 + 4\Lambda = 0. \tag{1.28}$$

This can be integrated to yield

$$C(r) = 2\ln\sigma + 2\ln\sin\left(\sqrt{2\Lambda}(r+R)\right), \tag{1.29}$$

with two integration constants, σ and R. We now shift the radial coordinate, removing thus R, and return to the metric ansatz to finally express the line element as

$$ds^2 = -dt^2 + dr^2 + dz^2 + \sigma^2\sin^2\left(\sqrt{2\Lambda}r\right)\, d\varphi^2. \tag{1.30}$$

The resulting magnetic field is

$$H(r) = \sqrt{\Lambda}\,\sigma\sin\left(\sqrt{2\Lambda}r\right). \tag{1.31}$$

This does not look like a constant field but we must bear in mind that this is just a coordinate expression and the measurable quantity, the Maxwell invariant, is constant since we find $F_{\mu\nu}F^{\mu\nu} = 2f^2 = 2\Lambda$.

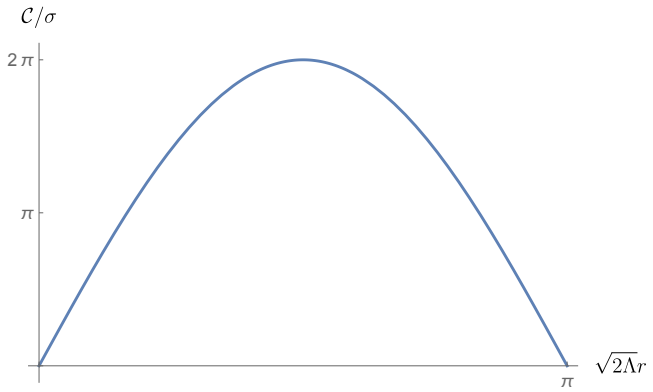

Figure 1.2: Circumference $\mathcal{C}$ of rings $t, z, r = \text{const.}$ in the homogeneous solution 1.30. Again, just like in the Bonnor–Melvin case, we observe two axes with a vanishing circumference.

The spacetime is obviously cyclic in the radial direction, so we may restrict the radial coordinate to $r \in [0, \pi/\sqrt{2\Lambda})$. As we approach the upper bound the circumference of the rings $t, z, r = \text{const.}$ vanishes which suggests this is the location of an axis of some sorts, see Figure 1.2. Perhaps a better picture is to think of the globe with geographical coordinates: φ then serves as the longitude while $\sqrt{2\Lambda}r$ is the latitude and our hoops are simply parallels or circles of latitude: we start with a point at the North Pole with $r = 0$, reach the longest hoop at the equator, and continue with shrinking rings all the way to the South Pole, see Figure 1.3.

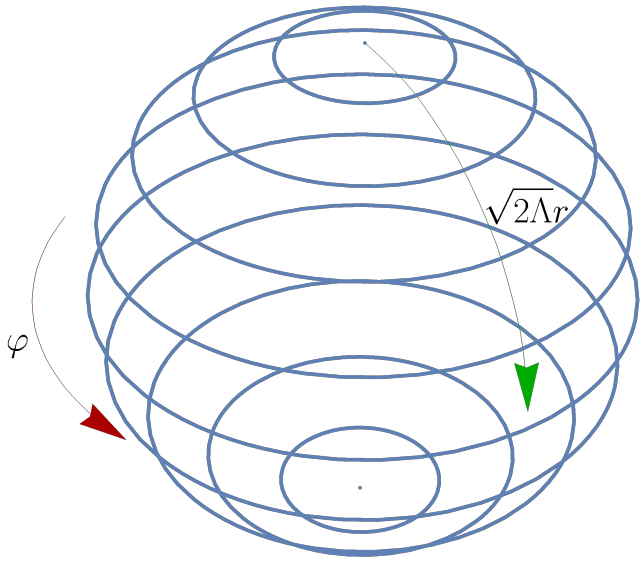

Figure 1.3: Representation of the spatial part of the homogeneous solution 1.30 depicting the hoops $t, z, r = \text{const.}$ in analogy with geographical coordinates.

To explore this in coordinates, we now rescale both r and φ to bring the line element into the form

$$ds^2 = -dt^2 + dz^2 + \frac{1}{2\Lambda}\left(dr^2 + \sin^2 r\, d\varphi^2\right), \tag{1.32}$$

with the corresponding change in the magnetic field

$$H(r) = \frac{1}{\sqrt{2}} \sin r. \tag{1.33}$$

Therefore, the resulting spacetime is locally a direct product of 2D Minkowski spacetime and a 2-sphere of constant radius $1/\sqrt{2\Lambda}$. These spacetimes have been explored by Plebański and Hacyan [14] and belong to the "exceptional electrovacuum type D metrics with cosmological constant", see also [6]. Generally, the solution has a deficit angle due to the presence of σ in (1.30) (the range of the angular coordinate in 1.32 is not $[0, \pi]$) and the axis is thus singular, forming the spacetime's only singularity. The spacetime is homogeneous and both charged and uncharged test particles can thus remain static anywhere or just sail along the magnetic field direction at a constant speed.

The studied situation is the best general relativistic approximation of the classical homogeneous magnetic field, including the behavior of test particles. But is this the only possible solution of the equations (1.18-1.21)? The answer is negative—the possible gravitational fields of cylindrically symmetric magnetic fields are much richer.

1.2 Special non-homogeneous magnetic field

Let us thus search for another solution of equations 1.18 to 1.21 that would involve a non-uniform magnetic field. This solution would depend on the value of the cosmological constant and perhaps some additional parameters and for a vanishing Λ, it should reduce to the Bonnor–Melvin solution 1.2 while it should include as a special case also the constant-field solution of [15]. Based on our previous discussion, one expects the solution to require a positive cosmological constant supporting the magnetic field against its own gravity and preventing it from collapsing upon itself. To simplify the problem at hand (which admits a large family of solutions as evidenced by solving the equations numerically, see below), we restrict to a subfamily featuring an additional symmetry—boost-symmetry along the cylindrical axis.[2] This amounts to the assumption $A = B$ and results in a warped product of a conformal 2D Minkowski and an additional 2D space [17]. Einstein equations then reduce substantially and we arrive at these relations

$$4ff'' - 7\left(f'\right)^2 - 4f^2(\Lambda - f^2) = 0 \tag{1.34}$$

for the magnetic field strength and

$$\exp A(r) = \exp B(r) = \frac{\alpha}{f(r)}, \tag{1.35}$$

$$\exp C(r) = \alpha\beta\frac{f'(r)^2}{f(r)^3}, \tag{1.36}$$

for the metric functions, with α, β integration constants. The last relation implies that we arrive at an axis wherever $f'(r) = 0$.[3] We can further shift the radial coordinate to put such an axis at $r = 0$. We thus ended up with a single second-order differential equation for $f(r)$, from which we are then able to determine the line element in a straightforward fashion. Let us now inspect the properties of 1.34 in more detail.

We claim that the solution is mirror-symmetric around any point with $f'(R) = 0$. Defining a new coordinate, ϵ, through $r = R + \epsilon$, the form of (1.34) remains unchanged. Now define another coordinate, $\bar{\epsilon}$, via $r = R - \bar{\epsilon}$. However, (1.34) still has the same form. Thus, with the

[2]Thus, in fact, the solution is boost-rotation symmetric but it is also static so that there is no gravitational radiation involved unlike in the general case reviewed in [16].

[3]Of course, we should also discuss the situation with $f(r) \to \infty$ or the fraction being indeterminate but this, in fact, is not the case for the actual solution.

same boundary conditions in both cases, the solution must be symmetric. The same boundary conditions mean the same value of f and its 1st derivative. But our assumption here is that f' vanishes so that it is the same in both directions indeed, rendering thus the solution mirror-symmetric.

Let us now rewrite (1.34) as follows

$$f'' = \frac{7}{4}\frac{(f')^2}{f} + f(\Lambda - f^2) \tag{1.37}$$

and assume $\Lambda > 0$ as expected. We integrate from the axis at $r = 0$, assuming without loss of generality that $f(0) > 0$.[4] If we start with $f(0) < \sqrt{\Lambda}$ then $f''(0) > 0$ and thus f starts growing until it overshoots Λ enough to reach $f''(0) = 0$ which then becomes negative until we get to a point where $f'(R) = 0$. This is the turning point with $f(R) > \Lambda$ and as per the argument above, the solution is again even, or mirror-symmetric, around $r = R$ so that it goes down again to reach the original value $f(0)$ and then the whole cycle repeats. The same argument can be used for $f(0) > \sqrt{\Lambda}$ only that the function now starts by decreasing until it necessarily reaches a minimum due to the first term in (1.37). In both cases, the solution is cyclic in r, featuring multiple axes. However, if the cosmological constant is negative the analysis along the lines above does not work and we cannot conclude anything about the periodicity of the solution.

One obvious exact solution results from $f(0)^2 = \Lambda > 0$, yielding $f(r)^2 = \Lambda$ everywhere—the homogeneous case of the previous section. Let us perturb this solution a little by assuming

$$f(r) = \sqrt{\Lambda}(1 + \varepsilon(r)), \tag{1.38}$$

with $\varepsilon(r) \ll 1$. To the lowest order, this gives a harmonic oscillator

$$\varepsilon'' + 2\varepsilon\Lambda = 0, \tag{1.39}$$

with the period $R = 2\pi/\sqrt{2\Lambda}$ and thus, $f(r) = \sqrt{\Lambda}(1 + \gamma\cos(\sqrt{2\Lambda}r))$ with $\gamma \ll 1$ and a shifted radial coordinate. For the metric coefficients, we get

$$\exp(A) = \exp(B) = \frac{\alpha}{\sqrt{\Lambda}(1 + \gamma\cos(\sqrt{2\Lambda}r))} \tag{1.40}$$

and

$$\exp(C) = 2\alpha\beta\gamma^2\sqrt{\Lambda}\frac{\sin^2(\sqrt{2\Lambda}r)}{(1 + \gamma\cos(\sqrt{2\Lambda}r))^3}. \tag{1.41}$$

Rescaling t and z, we set $\exp(A(0)) = \exp(B(0)) = \alpha/\sqrt{\Lambda}(1 + \gamma) = 1$. We further require elementary flatness of the axis, $g_{\varphi\varphi} = \exp C = r^2 + O(r^3)$, yielding

$$\frac{4\beta\gamma^2\Lambda^2}{(1 + \gamma)^2} = 1. \tag{1.42}$$

Therefore, once we specify the deviation from the constant solution, γ, the solution is unique. If we also demand that the other axis located at $r = \pi/\sqrt{2\Lambda}$ be regular without any deficit angle, we may write

$$-\frac{4\,(\beta\gamma^2(\gamma + 1)\Lambda^2)}{(\gamma - 1)^3} = 1, \tag{1.43}$$

[4] If $f(0) < 0$ we can absorb the changed sign in α in view of relations (1.35) and (1.36) so that it is always possible to choose $f > 0$.

which, however, together with 1.42, dictates $\gamma = 0$ and the perturbation vanishes. We conclude that near the homogeneous solution, there is a family of perturbed spacetimes but none of them is regular everywhere unlike the homogeneous one.

But can we do better? Perhaps we shall be able to find an exact solution to (1.37). We can see that it lacks r and we thus use f as the independent variable as our first step. We begin by setting $v = f'$ which produces $f'' = (f')' = \mathrm{d}v/\mathrm{d}r = (\mathrm{d}v/\mathrm{d}f)(\mathrm{d}f/\mathrm{d}r) = (\mathrm{d}v/\mathrm{d}f)v$, yielding

$$v(f)\frac{\mathrm{d}v(f)}{\mathrm{d}f} = \frac{7}{4}\frac{v(f)^2}{f} + f(\Lambda - f^2). \tag{1.44}$$

This relation can be converted to a linear equation by substituting $v^2 = w$ and thus $\mathrm{d}w/\mathrm{d}f = 2v(\mathrm{d}v/\mathrm{d}f)$ to get

$$\frac{1}{2}\frac{\mathrm{d}w}{\mathrm{d}f} = \frac{7}{4}\frac{w}{f} + f(\Lambda - f^2). \tag{1.45}$$

The general solution reads

$$wf^{-\frac{7}{2}} = \gamma - 4\sqrt{f} - \frac{4}{3}\Lambda f^{-\frac{3}{2}} \tag{1.46}$$

from which we derive

$$v = \frac{\mathrm{d}f}{\mathrm{d}r} = \pm\sqrt{\gamma f^{\frac{7}{2}} - 4f^4 - \frac{4}{3}\Lambda f^2} =: \pm\sqrt{\mathfrak{M}}, \tag{1.47}$$

where we defined a new function, the master function $\mathfrak{M}(f)$. Separating the variables and integrating, we can finally write

$$r = \pm\int \frac{\mathrm{d}f}{\sqrt{\mathfrak{M}}}. \tag{1.48}$$

This, in fact, is the inverse of the sought function $f = f(r)$. Returning to (1.36), we see that the roots of the square root in (1.47) determine where f' vanishes and thus they define the location of axes. Now, the integrand of (1.48) is real precisely between two subsequent roots $f' = 0$ where the argument of the square root is positive and, therefore, we always have two axes unless f vanishes there.

Since we are unable to evaluate the integral in 1.48, not even speaking of finding the inverse function, we use the gauge freedom again and instead of the original radial coordinate r, we shall use the density of the magnetic field f via (1.47). The relations (1.35) and (1.36) immediately yield closed-form expressions for all our metric functions

$$\mathrm{d}s^2 = \frac{1}{f}\left(-\mathrm{d}t^2 + \mathrm{d}z^2\right) + \frac{\mathrm{d}f^2}{\mathfrak{M}} + \beta\frac{\mathfrak{M}}{f^3}\mathrm{d}\varphi^2, \qquad \mathfrak{M} = \gamma f^{\frac{7}{2}} - 4f^4 - \frac{4}{3}\Lambda f^2, \tag{1.49}$$

where we rescaled the coordinates and repeated our definition of $\mathfrak{M}$ from above for the sake of clarity. The solution involves two integration constants, β and γ, and the cosmological constant, Λ. The electromagnetic field now is

$$F = \sqrt{\frac{\beta}{f}}\,\mathrm{d}f \wedge \mathrm{d}\varphi, \quad A = 2\sqrt{\beta f}\,\mathrm{d}\varphi. \tag{1.50}$$

The above solution is the main result of our paper [18]. We now turn to study its properties in more detail. Let us mention two special cases: first, if $\Lambda = 0$, we apply the transformation $f = 2K(1 - K^2r^2)^2$, redefine $\gamma = 4\sqrt{2K}$, and assume $\beta = 1/8K^3$ as required by the elementary

flatness of the axis—this yields the Bonnor–Melvin metric 1.2 as expected. And second, the value $\gamma = (16/3)\Lambda^{1/4}$ factorizing the master function $\mathfrak{M}$ corresponds to a single value $f^2 = \Lambda$ and yields the homogeneous solution 1.32 where f cannot be used as a coordinate since it has a constant value throughout the spacetime.

The spacetime is free of curvature singularities because the Kretschmann scalar is bounded for a finite f as is the actual case, see below. The most surprising fact about the solution is that it admits both signs of the cosmological constant since our original motivation and intuition was using a positive cosmological constant to balance the magnetic field against gravitational collapse.

To preserve the signature of the metric, we can only have a finite interval of f's between two subsequent roots of $\mathfrak{M}(f) = 0$ which implies $\gamma > (16/3)\Lambda^{1/4}$ for $\Lambda > 0$. The endpoints correspond to two axes since $g_{\varphi\varphi} = 0$ there, with the proper radial distance between them finite, making the spacetime radially compact and still a product of a warped Minkowski and a compact 2D space. For $\Lambda < 0$, any γ is fine, yielding a single finite interval $f \in [0; f_0]$ with $\mathfrak{M}(0) = \mathfrak{M}(f_0) = 0$, ensuring $\mathfrak{M} \geq 0$. The upper root represents an axis while $f = 0$ is, in fact, an asymptotic region since $g_{\varphi\varphi}$ diverges here and its proper distance from any other f is infinite. To the lowest order, we obtain for the asymptotic form of the spacetime

$$\mathrm{d}s^2 = \frac{1}{f}\left[\left(-\mathrm{d}t^2 + \mathrm{d}z^2\right) + \frac{\mathrm{d}f^2}{\frac{4}{3}|\Lambda|f} + \beta\frac{4}{3}|\Lambda|\mathrm{d}\varphi^2\right]. \tag{1.51}$$

Rescaling all coordinates, we see that this is the anti-de Sitter spacetime as expected due to the presence of a negative cosmological constant and the vanishing of the magnetic field.

The integration constants appearing in the solution are not independent if we further demand elementary flatness, or vanishing conicity, on the axes located at $f = f_i$, which requires

$$\sqrt{g_{\varphi\varphi}}(x) \approx \int_{f_i}^{x} \sqrt{g_{ff}(f)}\,\mathrm{d}f. \tag{1.52}$$

Taylor-expanding $\mathfrak{M}(f)$ near its root at $f = f_i$, which is always simple, we can write

$$\int_{f_i}^{x} \frac{\mathrm{d}f}{\sqrt{\mathfrak{M}'(f_i)(f - f_i)}} = 2\sqrt{\frac{f - f_i}{\mathfrak{M}'(f_i)}} = 2\sqrt{\frac{f - f_i}{2f_i(\Lambda - f_i^2)}}\,, \tag{1.53}$$

while the left-hand side of (1.52) gives

$$\sqrt{\frac{\beta}{f_i^3}\mathfrak{M}'(f_i)(x - f_i)} = \sqrt{\frac{2\beta}{f_i^2}(\Lambda - f_i^2)(x - f_i)}\,. \tag{1.54}$$

Combining these expressions, we fix one integration constant

$$\beta = \frac{f_i}{(f_i^2 - \Lambda)^2}. \tag{1.55}$$

If $\Lambda > 0$ we need to comply with the above equation for the two separate axes but $f_i = f_i(\Lambda, \gamma)$ so that (1.55) evaluated at both axes would produce two equations determining γ as well as β and the entire solution would be given in terms of Λ only. This, however, is not possible since the right-hand sides of the two copies of (1.55) are not independent for the two axes and, in fact, we cannot have both axes regular at the same time—one involves a conical defect. For a negative cosmological constant, we only have one axis to deal with and, therefore, β is determined in terms of γ, which remains a free parameter (or vice versa, of course), still ensuring a regular axis. Ultimately, the solution involves one free parameter in addition to the cosmological constant regardless of its sign.

1.3 General solution

We now return to the system (1.18)–(1.21) and examine the most general case of $A \neq B$. It turns out that the equations still can be separated in the following way. First, add (1.20) and (1.21) and substitute for $(A+B)'$ from (1.23) to yield

$$-2\frac{f''}{f} + 4\frac{(f')^2}{f^2} + 4(\Lambda - f^2) - \frac{C'f'}{f} = 0. \tag{1.56}$$

From here, we can express C' as follows

$$C' = -2\frac{f''}{f'} + 4\frac{f'}{f} + 4\frac{f}{f'}(\Lambda - f^2). \tag{1.57}$$

We now combine (1.18) + (1.19) − (1.20) − (1.21) to find

$$2C'' + (C')^2 - A'B' + 8f^2 = 0, \tag{1.58}$$

and express $A'B'$ from the resulting equation to substitute it together with (1.57) and (1.23) into (1.21) to obtain a single, separate, third-order equation for f

$$f'''f' - 2(f'')^2 + f''\left(6f(\Lambda - f^2) + \frac{(f')^2}{f}\right) + (f')^2(11f^2 - 9\Lambda) - 4f^2(\Lambda - f^2)^2 = 0. \tag{1.59}$$

We solve this equation and insert the solution into (1.57). We now know both f and C'. Writing (1.21) as $A'B' + (A+B)'C' + 4(\Lambda - f^2) = 0$, we substitute here for $(A+B)'$ from (1.23), which also yields $B' = -A' - 2f'/f$. We finally have a first-order equation for A, which is quadratic in A', and the same equation for B if we substitute for A instead. Its solution reads

$$A' = -\frac{f'}{f} \pm \sqrt{4\frac{f''}{f} - 7\left(\frac{f'}{f}\right)^2 - 4(\Lambda - f^2)}, \tag{1.60}$$

$$B' = -\frac{f'}{f} \mp \sqrt{4\frac{f''}{f} - 7\left(\frac{f'}{f}\right)^2 - 4(\Lambda - f^2)}. \tag{1.61}$$

Again, we determine f from (1.59), requiring 3 boundary conditions, and then we calculate A, B, and C from (1.60), (1.61), and (1.57), where we use the rescaling of t and z and the hoop length, so there are no additional integration constants. Next, we require a regular axis and a particular energy density of the magnetic field at a given location, leaving us with one free integration constant. Therefore, apart from the cosmological constant, the hoop length and field strength at a chosen point and one additional constant are the independent parameters of the solution.

If the square root in 1.60 and 1.61 vanishes, we obtain the previous, symmetric solution because this requirement is identical to 1.34. Since 1.59 does not involve the independent variable, we can now apply the same trick as for 1.37 and reduce the order of the equation by one as follows

$$v(f) = \frac{\mathrm{d}f(r)}{\mathrm{d}r} = f', \quad f'' = \frac{\mathrm{d}v(f)}{\mathrm{d}r} = \frac{\mathrm{d}f(r)}{\mathrm{d}r}\frac{\mathrm{d}v(f)}{\mathrm{d}f} =: v(f)\dot{v}(f),$$

$$f''' = v(v\ddot{v} + \dot{v}^2), \quad v(f)^2 =: w(f),$$
$$w\ddot{w} - \dot{w}^2 + \left[\frac{w}{f} - 6f\left(f^2 - \Lambda\right)\right]\dot{w} - 8\left(f^2 - \Lambda\right)^2 f^2 + 2w\left(11f^2 - 9\Lambda\right) = 0, \tag{1.62}$$

with dots denoting derivatives with respect to f. Since we do not have a readily available exact solution to this equation, we first attempt to linearize it near the exact solution 1.46. We thus assume that the solution is of the form $w(f) = \gamma f^{\frac{7}{2}} - 4f^4 - \frac{4}{3}\Lambda f^2 + \epsilon g(f)$ with ϵ controlling the order of approximation and plug this Ansatz into 1.62 to obtain, in the lowest order

$$\begin{aligned} 4f^2\left(-3\gamma f^{3/2} + 12f^2 + 4\Lambda\right)\ddot{g} - 24f\left(-3\gamma f^{3/2} + 11f^2 + 5\Lambda\right)\dot{g} \\ +7\left(-21\gamma f^{3/2} + 72f^2 + 40\Lambda\right)g = \ 0. \end{aligned} \tag{1.63}$$

Unfortunately, we have not been able so far to solve the above equation. Therefore, we now explore the numerical solutions of Einstein equations. Instead of the equation for f, we shall deal with the system 1.18–1.21 since it is more suited for a computer algebra system—the following plots have been generated using the *Maple* software. We fixed the boundary conditions at $r = 0$ and integrated until hitting a divergence of the system. This is not necessarily a physical singularity—if the physical field f has finite values—but a divergence of the calculated values which can be seen in the red curve of $C(r)$. We give here just four basic examples of behavior due to different boundary conditions. Let us briefly recall the form of our metric 1.7

$$ds^2 = -\exp A(r)\, dt^2 + dr^2 + \exp B(r)\, dz^2 + \exp C(r)\, d\varphi^2. \tag{1.64}$$

Functions A, B, and C thus determine the flow of time for static observers, distances along the axis, and the length of the hoops t, z, r = const., respectively. The numerical solutions can extend either indefinitely or end at a particular radial coordinate with an axis where the hoops shrink to a point ($C \to -\infty$) or an infinite hoop ($C \to +\infty$). Our exact solution 1.49 with $\Lambda > 0$, for instance, extends for a finite interval of the radial coordinate with two axes at its endpoints while it goes on to infinite radial distances for $\Lambda < 0$. The plots in Figure 1.4 are generated for boundary conditions specified at $r = 0$, without loss of generality, as the radial coordinate can be shifted arbitrarily. We can further choose any values for $A(0)$ and $B(0)$ since the corresponding coordinates, t and z, can be rescaled. Because the set of equations 1.18–1.21 only involves derivatives of the sought functions, fixing the value $C(0)$ only shifts $C(r)$ by a constant and we thus choose $C(0) = 0$. The boundary values for the derivatives $A'(0), B'(0)$, and $C'(0)$ were generated randomly so that we would get a real value of $f(0)$ from relation 1.21.

We can see that the possible structure of these spacetimes is quite rich and so our next step shall be to explore them in more detail, perhaps singling out a particular case admitting an exact solution. One of the questions to ask, for instance, is whether the exact solution 1.49 with $\Lambda < 0$ is the only one admitting infinite radial distances as seems to be the case from our numerical simulations.

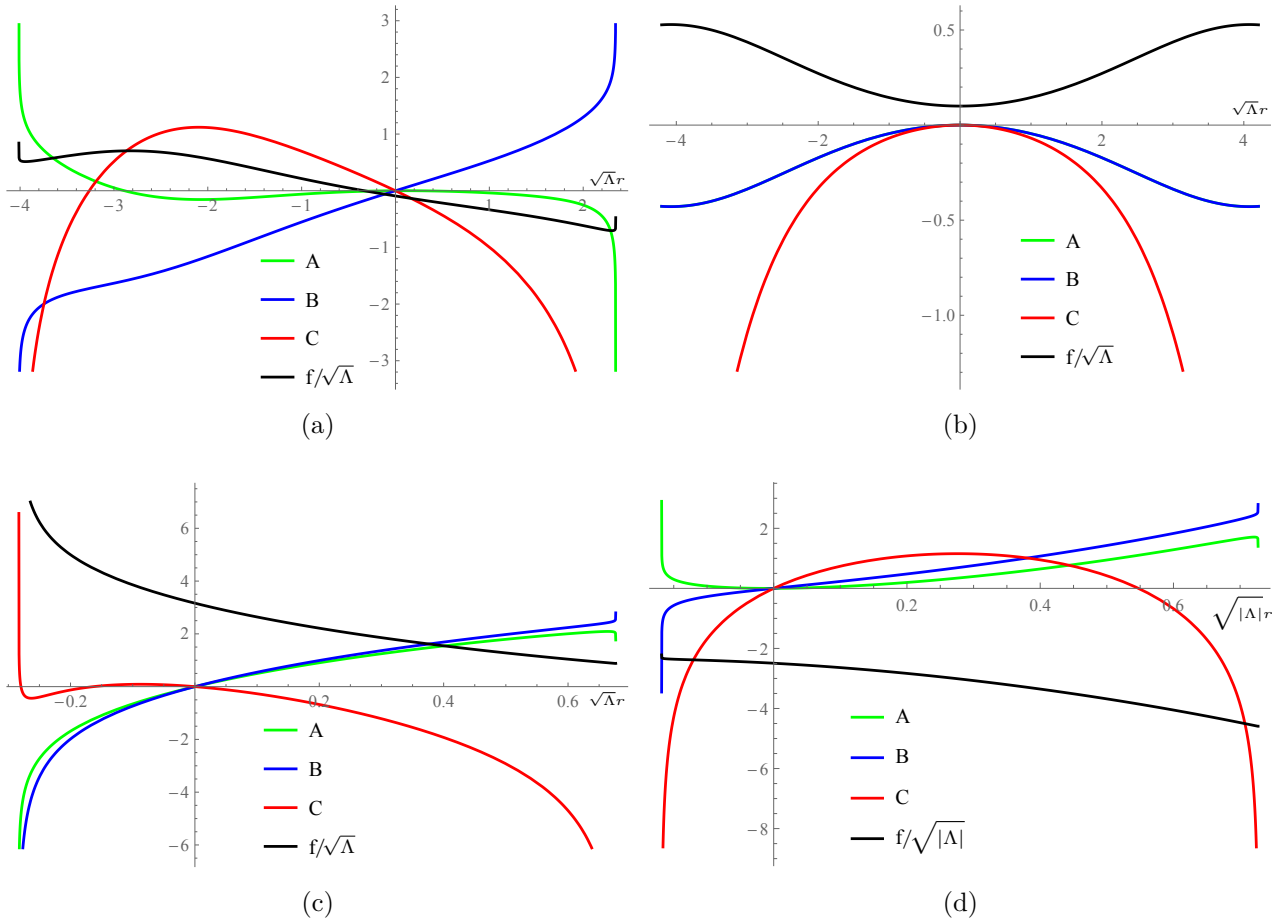

Figure 1.4: These are plots of numerically calculated metric components $A(r), B(r)$, and $C(r)$ (see the line element 1.64) and rescaled magnetic field strength $f(r)/\sqrt{\Lambda}$ as functions of rescaled radial cylindrical coordinate $\sqrt{\Lambda}r$. The first three plots feature a positive cosmological constant, while the last one has a negative Λ. This is a representation of four basic types of possible situations: (a) A solution involving two axes, $C \to -\infty$, with a finite proper distance between them. The axial and temporal directions are very different in terms of the behavior of the corresponding metric functions, A and B. The axis on the left is rather like a point, $B \to -\infty$, while the right axis stretches to infinity even locally, $B \to \infty$. Both axes are singular as the magnetic field diverges there, $f \to \infty$. (b) Two axes at a finite distance. The azimuthal and temporal directions are quite similar so that they overlap in the plot and the solution is almost boost-rotation symmetric like 1.49. There is no singularity in the spacetime. (c) An axis and an infinitely long hoop at a finite distance. The axial and temporal directions are rather similar again apart from the axis. The axial direction where the hoop lengths diverge shrinks to a point again, resembling rather a toroidal situation where the axial and azimuthal directions switch their meanings, and it is singular. (d) Two axes with no singularity; azimuthal and temporal directions dissimilar. The boundary conditions we used are specified in the text.

2 Spacetime crystals

Let us now turn to the question of adding solutions of Einstein equations—can we do it? In fact, the general answer is obvious since the equations are not linear so we lose the superposition principle of classical Newtonian gravitation. It is thus remarkable that there is a group of solutions to Einstein–Maxwell equations the members of which can be added with the sum still belonging to the same group. This is the Majumdar–Papapetrou family [19, 20] describing a general relativistic analog of static point masses with charges equal to their masses (we use Gaussian units with $4\pi\epsilon_0 = 1$) so that their electrostatic repulsion balances exactly their gravitational attraction. Amazingly, the classical situation translates to an exact, static, general relativistic solution! In four dimensions, we can write the metric element in the form

$$\mathrm{d}s^2 = -U^{-2}\mathrm{d}t^2 + U^2\mathrm{d}\vec{r}\cdot\mathrm{d}\vec{r}, \tag{2.1}$$

where the master function $U = U(\vec{r})$ is equal to the classical potential (up to a constant) generated by the point masses and the dot denotes the flat 3D scalar product. This is due to the fact that the entire set of Einstein–Maxwell equations reduces to a simple flat-space Laplace's equation $\Delta U(\vec{r}) = 0$ which is linear and identical to its classical counterpart. This extends not only to individual mass points as sources of otherwise vacuum fields but also to line and surface distributions of charge and even to charged dust. In this text, we focus on the first case only so that we can write

$$U(\vec{r}) = 1 + \sum_{i=1}^{N} \frac{Q_i}{\sqrt{(\vec{r}-\vec{r_i}).(\vec{r}-\vec{r_i})}}, \tag{2.2}$$

where r_i's are the positions of the individual points and Q_i's are their charges (and masses). While we can include an arbitrary constant in the potential of the classical theory without changing the physics, here it defines the "vacuum" situation with no charges present. We thus added unity to the potential in order to get an asymptotically flat spacetime as desired. If there is only a single point source the spacetime reduces to an extreme Reissner–Nordström solution describing an extremally charged black hole. As shown by Hartle and Hawking [21], this also happens if we add several charges—in general relativity, what was originally the position of the classical point source and what looked like a point is, in fact, a horizon of an extreme black hole of the RN type. As such, it is an example of a multi-black-hole spacetime.

We have previously explored the simplest possible case of two such black holes and discussed the behavior of test particles in their vicinity [22]. In our subsequent work [23], we studied another classical solution taken to the general relativistic arena—the field of an infinite charged string or straight line. As shown by Hartle and Hawking, there is necessarily a naked singularity enveloping non-point-like sources and this indeed is the case here. We then posed the question whether the spacetime of the extremally charged string, ECS, could be understood as a limit of a sequence of spacetimes due to discrete sources that would fuse together. This is the topic of the present section.

2.1 Like charges

To preserve the cylindrical symmetry of the ECS spacetime, it is obvious that the sought field must correspond to an infinite set of identical point charges distributed equidistantly along the

axis, ensuring thus axial symmetry and discrete translational symmetry along the axis. As is always the case in MP solutions, the spacetime is of course static, too. We are now ready to write down its master function in cylindrical coordinates, defining a new structure function φ as follows

$$U(\rho, z) =: 1 + \frac{Q}{k}\,\varphi(\rho, z), \tag{2.3}$$

while the general line element 2.1 still applies. Here, Q is the charge (and mass) of the separate sources and k is the distance between neighboring points, or lattice constant. Using dimensionless coordinates rescaled by k from now on, we cast the structure function into the form

$$\varphi(\rho, z) = \frac{1}{\sqrt{\rho^2 + z^2}} + \sum_{n=1}^{\infty}\left[\frac{1}{\sqrt{\rho^2 + (z-n)^2}} + \frac{1}{\sqrt{\rho^2 + (z+n)^2}} - \frac{2}{n}\right]. \tag{2.4}$$

We took out the point at the origin of coordinates and summed over pairs of points at equal distances from the origin. Further, we subtracted the standard term $2/n$ to ensure convergence of the non-local part of the potential near the origin. We now need to address two issues: Can we find a closed form for the infinite sum above? And does the sum actually solve Laplace's equation?

The first question is, in fact, rather simple to answer—no, we can not, unfortunately. We are thus to deal with infinite sums throughout our investigation, emphasizing the importance of the second issue above. Therefore, we must investigate the convergence properties of the structure function 2.4. But before we do so, let us discuss the periodicity of the potential. We can write

$$\varphi(\rho, z+1) = r_{-1} + \sum_{n=1}^{\infty}\left(\frac{1}{r_{n-1}} + \frac{1}{r_{-n-1}} - \frac{2}{n}\right), \tag{2.5}$$

where we used a new shorthand notation $r_n = \sqrt{\rho^2 + (z-n)^2}$ for the distance of a given point (ρ, z) from the n-th lattice point on the axis. We take some terms out of the sum, rewrite it using a new summation index, and insert and subtract $2/l$. This turns the above expression for $\varphi(\rho, z+1)$ into

$$\frac{1}{r_0} - 1 + \frac{1}{r_1} - \frac{1}{2} + \sum_{l=2}^{\infty}\left(\frac{1}{r_l} + \frac{1}{r_{-l}} - \frac{2}{l}\right) + \sum_{l=2}^{\infty}\left(\frac{2}{l} - \frac{1}{l+1} - \frac{1}{l-1}\right). \tag{2.6}$$

The last sum cancels with $-1/2$ and we get

$$\varphi(\rho, z+1) = \frac{1}{r_{-1}} - 1 + \frac{1}{r_0} + \frac{1}{r_1} - 1 + \sum_{l=2}^{\infty}\left(\frac{1}{r_l} + \frac{1}{r_{-l}} - \frac{2}{l}\right) = \varphi(\rho, z). \tag{2.7}$$

This shows that the potential has a period 1 in z. We now proceed to discuss the convergence properties of the potential. We first notice that on the axis, the sum has a closed form

$$\varphi(0, z) = \frac{1}{|z|} - H(z) - H(-z), \tag{2.8}$$

where $H(z)$ is the harmonic number[1]. We would like to establish uniform convergence of the series so we need a bound independent of ρ and z. We find $1/r_n + 1/r_{-n} - 2/\sqrt{n^2} \sim 1/n$ but

[1]The harmonic number is defined as $H(z) = \gamma + \psi(z+1)$, with $\psi(z) = \frac{1}{\Gamma(z)}\frac{\mathrm{d}\Gamma(z)}{\mathrm{d}z}$ the digamma function and γ the Euler-Mascheroni constant, see [24].

this is not sufficient. Restricting to the strip $0 \leq z \leq 1/2$, let us now look at the derivatives of the individual potential components for $n \geq 1$. We find

$$0 \leq \frac{\partial}{\partial z}\left(\frac{1}{r_n}\right) \leq \frac{4}{(2n-1)^2}, \qquad -\frac{8}{3\sqrt{3}(2n-1)^2} \leq \frac{\partial}{\partial \rho}\left(\frac{1}{r_n}\right) \leq 0 \tag{2.9}$$

and

$$-\frac{1}{n^2} \leq \frac{\partial}{\partial z}\left(\frac{1}{r_{-n}}\right) \leq 0, \qquad -\frac{2}{3\sqrt{3}n^2} \leq \frac{\partial}{\partial \rho}\left(\frac{1}{r_{-n}}\right) \leq 0. \tag{2.10}$$

Using the triangle inequality, we then conclude

$$\left|\frac{\partial}{\partial z}\left(\frac{1}{r_n}+\frac{1}{r_{-n}}\right)\right| \leq \frac{8n^2-4n+1}{n^2(2n-1)^2}, \qquad \left|\frac{\partial}{\partial \rho}\left(\frac{1}{r_n}+\frac{1}{r_{-n}}\right)\right| \leq \frac{2\,(8n^2-4n+1)}{3\sqrt{3}n^2(2n-1)^2}. \tag{2.11}$$

This is already sufficient as the corresponding series converge in both cases and we thus have uniform absolute-convergence for the derivatives of the series in (2.4) (the same applies to higher derivatives of the series). We also know that the series itself converges along the axis, which implies it converges locally uniformly within the strip $z \in [0, 1/2]$ and we can exchange the summation and derivatives, $\nabla_\mu \nabla_\nu \sum_{n=1}^{\infty}\left[\frac{1}{r_n}+\frac{1}{r_{-n}}-\frac{2}{n}\right] = \sum_{n=1}^{\infty} \nabla_\mu \nabla_\nu\left[\frac{1}{r_n}+\frac{1}{r_{-n}}-\frac{2}{n}\right]$. We have thus shown that the above series satisfies Laplace's equation here. Adding the term $1/r_0$ and using the symmetries of the potential it then follows that the full potential is a solution of Laplace's equation throughout the entire space save for the punctures—the lattice points along the axis. For details, we refer the reader to [25].

We present several plots of the resulting potential in Figure 2.1 below. One of the obvious features in subplot (a) are the divergences located at the punctures and at the cylindrical radial infinity $\rho \to \infty$. The divergences, however, do not signal any physical singularities where the scalars describing the spacetime would diverge—these in fact occur where the Maxwell invariant, $F_{\alpha\beta}F^{\alpha\beta} = -2(\nabla U)^2/U^4$, diverges. We must thus look at locations of a vanishing U instead. It then follows from 2.3 that the singularities occur at equipotential surfaces defined by the relation $\varphi(\rho, z) = -k/Q$. This is precisely what we plotted in 2.1(b)–(d). For each of these surfaces we can always find the corresponding charge so that the surface is singular. The disjoint singularities only occur for positive values of the potential that require a negative charge of the black holes, which entails a negative mass as well. Note that the surface area of the singularities vanishes due to the metric form 2.1 so that they are actually points and not extended surfaces as they seem to be in our cylindrical coordinates. This extends the observation by Hartle and Hawking [21] and shows there can be a naked singularity even for discrete sources. When we examine the metric near the punctures, we discover that it is regular and the punctures are, in fact, not points but spheres of a finite surface $4\pi Q^2$—horizons of extreme Kerr–Newman-type black holes [26]. The situation is identical to a finite number of MP black holes discussed in [21] where we can continue through the horizon to a singularity inside it.

What does the solution look like far away from the axis? Let us inspect the derivatives of the potential. We notice that $(1/r_n + 1/r_{-n})_{,\rho}$ are negative and increasing functions of n so that we can use integral estimates of the series to find

$$\left(\frac{1}{r_0}\right)_{,\rho} + \left(\frac{1}{r_1}+\frac{1}{r_{-1}}\right)_{,\rho} + \int_1^\infty \left(\frac{1}{r_n}+\frac{1}{r_{-n}}\right)_{,\rho} \mathrm{d}n \leq \frac{\partial \varphi}{\partial \rho} \leq \left(\frac{1}{r_0}\right)_{,\rho} + \int_1^\infty \left(\frac{1}{r_n}+\frac{1}{r_{-n}}\right)_{,\rho} \mathrm{d}n. \tag{2.12}$$

The integrals can be easily evaluated and combined with the corresponding asymptotic series to obtain

$$-\frac{2}{\rho} - \frac{1}{\rho^2} + \frac{3z^2+4}{2\rho^4} + O\left(\frac{1}{\rho^5}\right) \leq \frac{\partial \varphi}{\partial \rho} \leq -\frac{2}{\rho} + \frac{1}{\rho^2} - \frac{3z^2+2}{2\rho^4} + O\left(\frac{1}{\rho^5}\right). \tag{2.13}$$

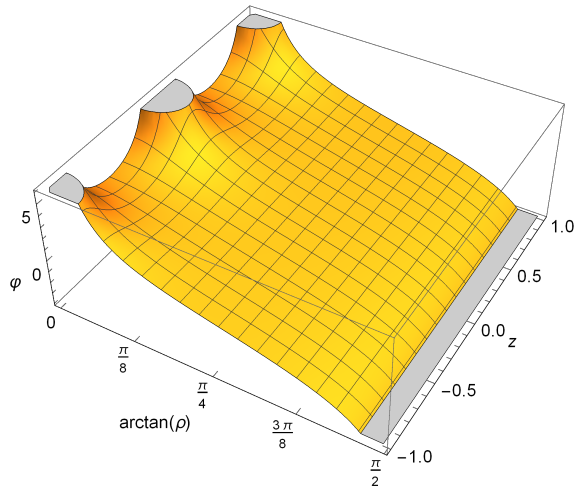

(a) Potential φ of 2.4 for $\rho \in [0, \infty)$ (notice the rescaled radial coordinate).

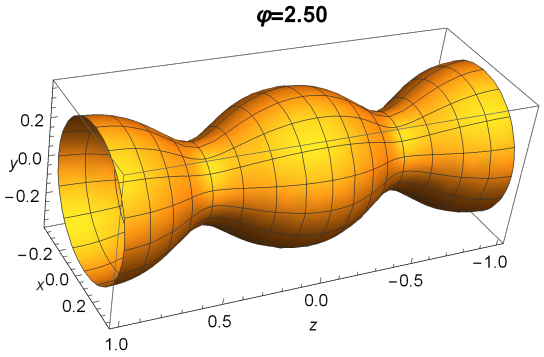

(b) An equipotential surface of φ with a single outer singularity. We can see the rotational symmetry around the axis and the discrete translational symmetry along it.

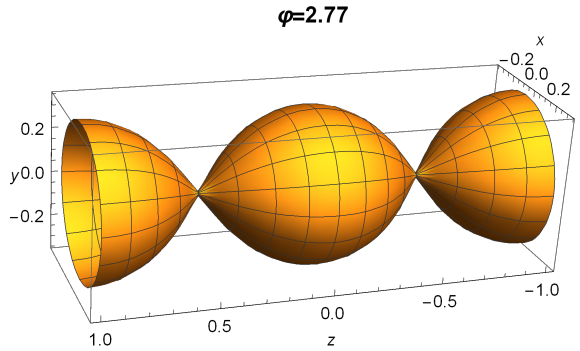

(c) The borderline case of a simply connected outer singularity.

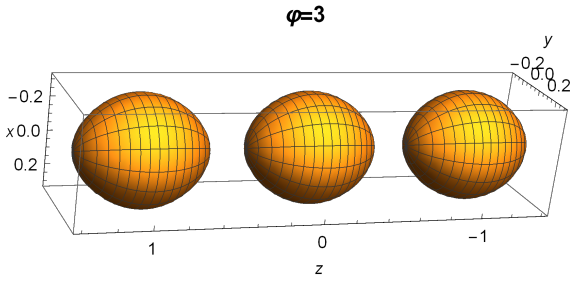

(d) A disconnected set of separate outer singularities.

Figure 2.1: Numerical plots of the potential 2.4. In (a), we notice divergences at the punctures and at radial cylindrical infinity. The remaining plots are equipotential surfaces of the potential, defining the position of the physical singularity for $-k/Q$ equal to the given value, see the main text for further details.

It then follows that $\varphi_{,\rho} \to 0$ for $\rho \to \infty$. More precisely, $\varphi_{,\rho} \sim -2/\rho$ and thus $\varphi \sim -2 \ln \rho$. We can also see that for large ρ the dependence on z vanishes as expected, confirming thus the existence of an asymptotic axial Killing vector. Both these facts are consistent with the ECS spacetime [23] and the leading-order asymptotics in ECS and the present spacetime are thus identical far away from the axis.

A natural question to ask now concerns the behavior of test particles—both uncharged and charged ones. A general solution is impossible due to the form of the metric so we instead pay attention to some paths of physical interest. There are points of obvious symmetry located at the centers between two neighboring punctures where any test particle can remain static indefinitely. It is quite interesting that a particle with a specific charge $q = Q/M$ equal to that of the black holes that generate the spacetime—i.e., ± 1 and thus actually an object of the same features as the field sources but not deforming the spacetime itself—can remain static anywhere. We just mention here circular electrogeodesics, which only exist within the symmetry planes

$z = 0$, $z = 1/2$, and their mirror images. There are circular photon paths located at the roots of $U + 2\rho U_{,\rho} = 0$. Charged massive particles move along circular electrogeodesics at an angular frequency of

$$\omega^2 := \left(\frac{\mathrm{d}\phi}{\mathrm{d}\tau}\right)^2 = \frac{2(1-q)Q}{k\rho^2} + O\left(\frac{Q^2}{k^2}\right), \tag{2.14}$$

with τ their proper time. Compared with ECS electrogeodesics [23], we see that asymptotically, the source is again compatible with linear mass and charge density of Q/k. Since we gain the Killing field $\partial/\partial z$ here, we also have asymptotic helical paths winding along the axis.

2.2 Unlike charges

We were able to determine the asymptotic form of the positive "crystal" spacetime and compare it to the field of a charged string—we concluded that it diverges far away from the axis. Can we perhaps modify our sources in such a way that the spacetime would be cylinder-asymptotically flat, which is more desirable and interesting? This would certainly require negative masses as, in essence, the total mass of the source must vanish. We thus construct a crystal similar to the previous case but with sources of alternating signs of electric charges—and thus also of masses. We still have a metric of the form 2.1 but the structure function is now modified

$$U(\rho, z) = 1 + \frac{Q}{k}\sum_{n=-\infty}^{\infty}\frac{(-1)^n}{\sqrt{\rho^2 + (z-n)^2}} := 1 + \frac{Q}{k}\,\chi(\rho, z). \tag{2.15}$$

The period of the structure function is $2k$ now but, unlike in the previous case, the potential is also antiperiodic with antiperiod k. Its convergence properties are better and we have shown in [25] that the above sum and sums of the corresponding first and second derivatives converge uniformly throughout the domain apart from the punctures so that χ and thus also U are solutions of Laplace's equation, ensuring that this is indeed a solution of Einstein–Maxwell equations as well. See Figure 2.2 for a plot of the potential. The singularities now only envelop every second puncture—sources of positive mass—and they are thus never connected. For negative punctures, there are no horizons at the lattice points and, instead, there is a singularity hidden on the other side, which is not covered by our cylindrical coordinate system.

Let us now inspect the asymptotics of the spacetime as $\rho \to \infty$. Using the same arguments as for the uniform crystal, we arrive at a relation

$$-\frac{2}{\rho^2} + \frac{6z^2+17}{2\rho^4} + O\left(\frac{1}{\rho^5}\right) \leq \frac{\partial\chi}{\partial\rho} \leq \frac{2}{\rho^2} - \frac{6z^2+13}{2\rho^4} + O\left(\frac{1}{\rho^5}\right). \tag{2.16}$$

We thus conclude that $\chi_{,\rho} \sim \rho^{-2}$ or faster. Can we improve this estimate? It turns out we can, using an expansion in the fundamental solutions of Laplace's equation in cylindrical coordinates—the Bessel functions. We assume the potential in the form of a sum of separated modes

$$\chi \sim \sum_{n=1}^{\infty} A_n(z)B_n(\rho), \tag{2.17}$$

where every mode satisfies Laplace's equation, leading to

$$-\alpha_n^2 = \frac{A_n''(z)}{A_n(z)} = -\frac{1}{B_n(\rho)}\left(B_n''(\rho) + \frac{B_n'(\rho)}{\rho}\right). \tag{2.18}$$

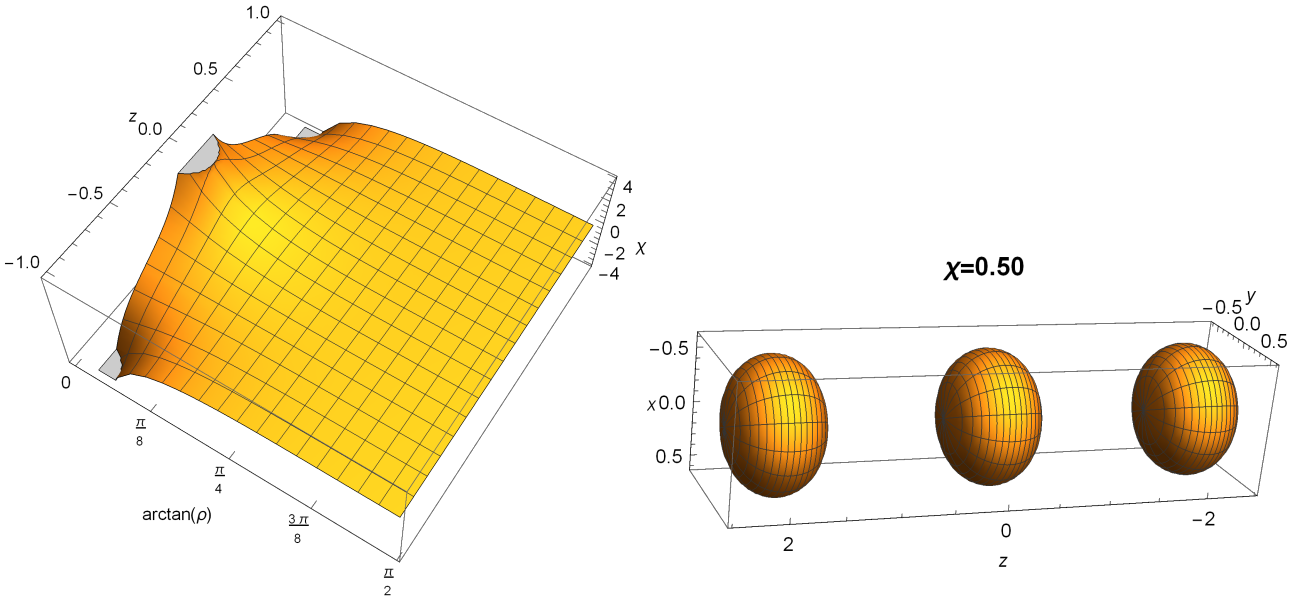

(a) A numerical plot of the potential χ of 2.15.

(b) An equipotential surface of the potential.

Figure 2.2: The potential diverges to $\pm\infty$ at the punctures while it vanishes asymptotically. The equipotential surfaces determining the position of singularities are always disconnected since the potential χ vanishes at midsurfaces between neighboring punctures with $z = 1/2 \pm n$.

Here we already assumed z-periodicity of the solution in choosing the correct sign of the separation constant. We can thus write each mode as a product of the form

$$[a_n \sin(\alpha_n z) + b_n \cos(\alpha_n z)]\,[c_n I_0(\alpha_n \rho) + d_n K_0(\alpha_n \rho)]\,.$$

The potential χ is reflection symmetric, $\chi(z) = \chi(-z)$, so that $a_n = 0$ while its anti-periodicity yields

$$A_n(z+1) = -A_n(z) \Rightarrow \cos(\pi n) = -1 \Rightarrow n = 1, 3, 5, \ldots \tag{2.19}$$

Lastly, we know that I_0 diverges at $\rho \to \infty$ and thus we require $c_n = 0$. Using Gauss's law to compare the sources of the potential 2.17 to the electric charges distributed along the axis, we finally arrive at the expression

$$\chi = 4 \sum_{l=1}^{\infty} \cos\left[\alpha_l z\right] K_0\left[\alpha_l \rho\right], \quad \alpha_l = \pi(2l-1). \tag{2.20}$$

Returning now to the asymptotic behavior of the potential 2.16, we use the leading-order term for the Bessel function and since the dependence on z vanishes asymptotically, we express the potential in the plane $z = 0$ to obtain

$$\chi = \sum_{l=1}^{\infty} 4\sqrt{\pi} e^{-\alpha_l \rho} \left(\frac{1}{\sqrt{2\alpha_l \rho}} + O\left(\frac{1}{(\alpha_l \rho)^{3/2}} \right) \right). \tag{2.21}$$

The sum has no closed formula, but we can get a lower and upper integral estimates as follows, omitting the higher-order terms

$$\frac{\sqrt{2}}{\pi} \frac{e^{-\pi\rho}}{\rho^{3/2}} \leq \chi \leq 2\sqrt{2} \frac{e^{-\pi\rho}}{\rho^{1/2}}. \tag{2.22}$$

Numerical evaluation finally suggests $\chi \approx 2.74 e^{-\pi\rho}\rho^{-1/2}$, which is close to the upper estimate. The exponential decay of the master function with radial distance from the axis means that the spacetime is radially asymptotically flat and it approaches Minkowski faster than for any isolated system. Applying the same procedure to the uniform crystal, we find $\varphi = -2\ln\rho + 4\sum_{l=1}^{\infty}\cos[\alpha_l z]\,K_0[\alpha_l\rho]$ with $\alpha_l = 2\pi l$. Taking now the limit $k \to 0^+$ with Q/k constant, the entire spacetime apart from the axis gets squashed to form the radial cylindrical infinity of the ECS spacetime as expected intuitively.

As we have shown above, it is possible to work with the infinite sums to some extent but, on the other hand, it would be much more comfortable to work with closed-form expressions instead. To this end, we now proceed to obtain a similar crystal-like 4D structure from a very different starting point.

2.3 Dimensional reduction

We now take advantage of three important facts: the Majumdar–Papapetrou class can be generalized to higher dimensions, some of these spacetimes with an infinite number of sources can be cast in a closed form, and higher-dimensional solutions of symmetry can be reduced to spacetimes of a lower number of dimensions.

Let us begin by giving the form of the MP solution in an arbitrary dimension $D = n+1 \geq 4$ (see [27, 28])

$$ds^2 = -U^{-2}\mathrm{d}t^2 + U^{\frac{2}{n-2}}\delta_{ij}\mathrm{d}x^i\mathrm{d}x^j, \tag{2.23}$$

where i, j range from 1 to n and t is a time-like Killing coordinate, so that the metric is static with the function $U = U(x^i)$ only depending on the Cartesian-like spatial coordinates x^i. The spatial part of the metric is conformally flat. The electromagnetic potential A and electromagnetic field tensor F read

$$A = c_n\frac{\mathrm{d}t}{U}, \quad F = \mathrm{d}A = -c_n\sum_{i=1}^{n}\frac{U_{,i}}{U^2}\mathrm{d}x^i \wedge \mathrm{d}t, \tag{2.24}$$

with $c_n = \sqrt{\frac{n-1}{2(n-2)}}$. The particular 5D solution we are interested in is again the field of an infinite number of black holes distributed regularly along the axis with a separation constant k and charge and mass Q:

$$\mathrm{d}s^2 = -U^{-2}\mathrm{d}t^2 + U\left(\mathrm{d}\rho^2 + \rho^2\mathrm{d}\phi^2 + \rho^2\sin^2\phi\;\mathrm{d}\xi^2 + \mathrm{d}z^2\right), \quad A = \frac{\sqrt{3}}{2}\frac{\mathrm{d}t}{U}, \tag{2.25}$$

with

$$U(\rho, z) = 1 + \frac{Q}{k^2}\sum_{n=-\infty}^{+\infty}\frac{1}{\rho^2 + (z-n)^2} := 1 + \frac{Q}{k^2}\,\eta(\rho, z), \tag{2.26}$$

where we use dimensionless hypercylindrical coordinates rescaled by k and define a new structure function η. Now comes the magical second step: in odd dimensions, the sum has a closed form! In our 5D case, we can write

$$\eta(\rho, z) = \frac{\pi}{\rho}\frac{\sinh(2\pi\rho)}{\cosh(2\pi\rho) - \cos(2\pi z)}. \tag{2.27}$$

We now reduce the solution to 4D following the standard procedure, see [29], where we take advantage of the fact that the metric is independent not only of the temporal and azimuthal coordinates t and ϕ but also of the additional 5D coordinate ξ. The resulting metric reads

$$\mathrm{d}s^2 = -U^{-2}\mathrm{d}t^2 + U\left(\mathrm{d}\rho^2 + \rho^2\mathrm{d}\phi^2 + \mathrm{d}z^2\right). \tag{2.28}$$

This, however, comes at a twofold cost—in addition to the electromagnetic field, there is now a scalar field as well, which also contributes to the gravitational field. It is of interest that the field itself is not axially symmetric, providing thus an example of a matter field not sharing the symmetries of the gravitational field it co-generates:

$$\Phi(\rho, \phi, z) = \sqrt{U}\rho\sin\phi. \tag{2.29}$$

The corresponding equation governing the scalar field is

$$3\Box\Phi = \Phi R. \tag{2.30}$$

Further—and this needs to be emphasized—the resulting structure function now satisfies a modified equation, namely

$$U_{,\rho\rho} + U_{,zz} + 2\frac{U_{,\rho}}{\rho} = 0, \tag{2.31}$$

which is not Laplace's equation. Put differently, the spacetime is not a solution of Einstein–Maxwell equations but of a modified set. In fact, Einstein equations still have the same form with stress-energy tensors of the electromagnetic and scalar fields on the right-hand side. However, Maxwell equations are modified now and read $\nabla_\beta\left(\Phi F^{\alpha\beta}\right) = 0$. On the other hand, the solution has two nice features—there are no singularities (the punctures are horizons again) and the spacetime is cylindrically asymptotically flat with $\eta \sim \pi/\rho$. Its main advantage though consists in the fact that it is expressed in a closed form so that we can study its features analytically. For instance, it is straightforward to calculate trajectories of charged test particles. In particular, asymptotic circular electrogeodesics yield

$$\omega^2 = \frac{\pi Q}{k^2\rho^3}\left(1 - \frac{\sqrt{3}}{2}q\right) + O\left(\frac{Q^2}{k^4}\right). \tag{2.32}$$

We see that far away from the axis the source behaves as a Reissner–Nordström point source of mass $\pi Q/k$ and charge $\sqrt{3}\pi Q/(2k)$. The leading order in ω^2 is ρ^{-3} because of the asymptotic flatness and presence of the scalar field Φ. The specific charge of the black holes thus complies with that of static test particles, which must have $q^2 = 4/3$.

In conclusion, we have succeeded in creating three different models of a spacetime featuring a discrete local symmetry that goes over to a Killing vector field asymptotically. The three scenarios discussed above all have their advantages and drawbacks as we have pointed out. In our future work we plan on using these solutions as a starting point for various averaging techniques used in cosmology to see whether they indeed reproduce the asymptotic symmetry as expected. Another topic we intend to discuss are perturbations of these exact spacetimes—it is well-known that MP solutions admit rather simple perturbations in terms of slow motion of the sources. A natural question to ask is under what conditions would we get a collapse? And would the collapse produce apparent horizons? This seems to be quite an interesting field to investigate in the future.

3 Spacetime locomotion

In the present chapter, we shall discuss an interesting possibility of controlled motion through a gravitational field without using any reactive propulsion. One can think of a child swinging on a hanging seat—through periodic and well timed crouching and sitting upright, they can increase their energy and reach ever higher points until they go all the way around [30]—at which point their parents go round the bend, too! Here in fact, the child-swing system interacts with the Earth and exchanges internal chemical energy stored in the child for the total mechanical energy of the child-swing system. The gravity-assist or gravitational-slingshot trajectories of interplanetary space probes use the same swinging technique with the interaction ensured by the gravitational attraction [31]. But can we do without the Earth and the planets and use only the gravitational field itself? The answer is affirmative and relies upon working with extended bodies moving through the field.

The Newtonian effects mentioned above are usually referred to as "swinging" to distinguish them from the general relativistic effect of "swimming" whereby a non-point-like test body changes its position in or motion through spacetime by performing cyclic changes in its configuration similarly to a swimmer performing a stroke—hence the name [32]. We must emphasize though that the two effects go hand in hand and the Newtonian effect obviously needs to be included in general relativity as well since we must obtain it in the Newtonian limit of the general case. The passive effect of this type can be observed, for instance, in the long-term changes of the Moon's orbit due to its tidal deformations and transfer of Earth's rotational into Moon's orbital energy, pushing it ever farther away from the Earth [33]. However, we are interested in an active change of the object's path. In fact, there have already been in-orbit experiments [34] performed with satellites releasing masses attached on long strings to see whether this could be used to stabilize orientation of the probes or even change their trajectory. To reduce this complicated problem, we shall discuss the motion of a dumbbell-like body consisting of two equal point masses connected via a massless rod of a length that changes in a predetermined manner given as a specific function of time [35, 36, 37, 38]. If this indeed works—that is, if the dumbbell is able to "climb" in a gravitational field—then it will be an example of a reactionless drive, which is pushing against nothing at the expense of some internal energy stored in the system.

3.1 Swimming dumbbells?

To be precise, we shall study a dumbbell system moving radially in the field of a Schwarzschild black hole of mass M, following a previous paper [39]. Our goal is to verify and perhaps extend the results presented in this work, which claimed to have confirmed the swimming effect. The system is described by the following relativistic Lagrangian formed as a sum of Lagrangians for the individual particles forming the ends of the dumbbell

$$L_d = -m\sqrt{1-\frac{2M}{r}-\frac{\left(\frac{\mathrm{d}r}{\mathrm{d}t}\right)^2}{1-\frac{2M}{r}}}-m\sqrt{1-\frac{2M}{r+l}-\frac{\left(\frac{\mathrm{d}r}{\mathrm{d}t}+\frac{\mathrm{d}l}{\mathrm{d}t}\right)^2}{1-\frac{2M}{r+l}}}, \tag{3.1}$$

where we use the standard Schwarzschild coordinates r and t and $l(t)$ determines how the dumbbell expands and contracts with time

$$l(t) = \frac{\delta l}{2}(1 - \cos\left[2\pi\omega t\{\alpha(1-\omega t), +1\}\right]), \tag{3.2}$$

here, the parameter α defines whether the dumbbell first stretches slowly to shrink quickly ($\alpha < 0$), or whether it first expands hastily to then contract gently ($\alpha > 0$), see Figure 3.1. The sign of α generally splits the dumbbell swimmers into two broad groups that yield different results, see below. The frequency parameter ω sets the typical time scale of the problem and determines the time it takes the dumbbell to shrink to a single point again.

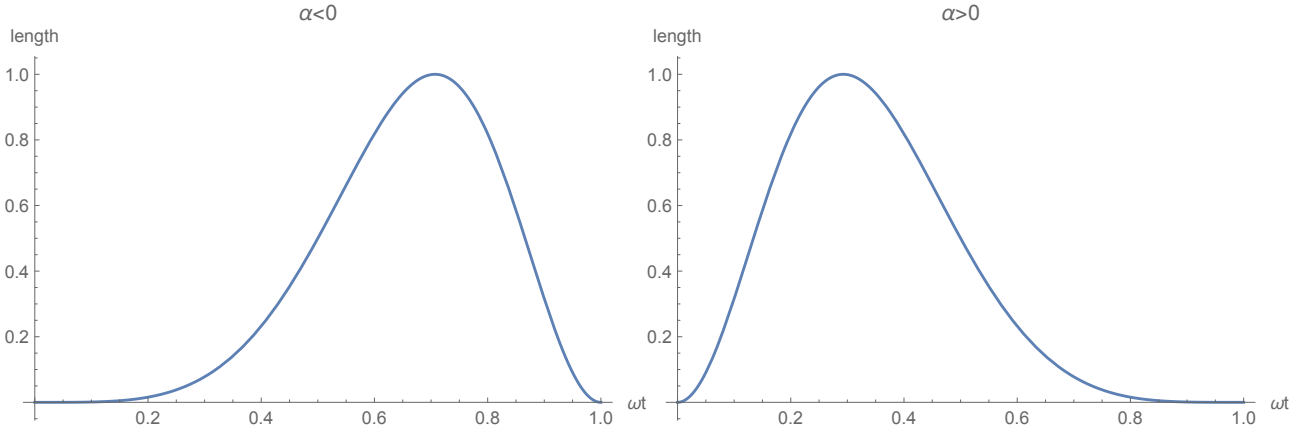

Figure 3.1: One cycle of expansion and contraction of the test dumbbell as given by 3.2. Left, slow expansion and fast contraction corresponding to $\alpha < 0$ and right, the opposite behavior for $\alpha < 0$.

In fact, the original paper [39] used a different deformation function but claimed that their results were robust and broadly independent of the deformation function. We verified this and chose a different swimming stroke since their function was not analytic at the endpoints of the dumbbell evolution, which turned out to be a major problem when extending the range of frequencies in our calculations.

It remains to be seen whether the above setup describes a physically acceptable system or whether we need to choose a completely different starting point to define our system. In fact, we are basically trying to find a model of a robotic spring that performs a preset swimming stroke as it falls in the gravitational field—this is closely related to the rich field of the so-called controlled lagrangian systems that deal with robots navigating various surroundings, refer to, e.g., [40, 41, 42]. But as we shall see below this can be dubious in general relativity.

We let the dumbbell fall freely from rest at a given initial distance from the black hole expressed in terms of the spherical radial coordinate. The task of the dumbbell is to slow down or perhaps even reverse its fall as compared to a simple point mass falling with the same initial conditions. We follow its progress throughout its motion by monitoring the difference between the position of the geometric center of the dumbbell and the location of the reference particle

$$\delta r(t) = r(t) + \frac{l(t)}{2} - r_p(t). \tag{3.3}$$

The shift, $\delta r(t)$, closely follows the shape of the deformation function 3.2. However, we only focus on the final shift after the dumbbell completes a full stroke. We thus wait until the

dumbbell contracts back to a point and then evaluate the shift δr, which is no longer a function of time and depends solely on the oscillation frequency ω (with a fixed maximum length δl). We find that the particular form of the deformation function is not of essence and the dumbbell indeed behaves in a similar way depending just on the general deformation shape of Figure 3.1. To show that the effect is present in the Newtonian case too, we first calculated the dumbbell motion in the classical field of a point mass M, see Figure 3.2. Although our Lagrangian 3.1, and particularly its Newtonian version, is deceptively simple, it is impossible to integrate the resulting equations of motion analytically and we must resort to numerical computations for which we used the computer algebra systems *Maple* and *Mathematica*. Our results presented here use the same initial conditions of a dumbbell shrunk to a single point and falling from rest at the initial distance of $r_0 = 120M$.

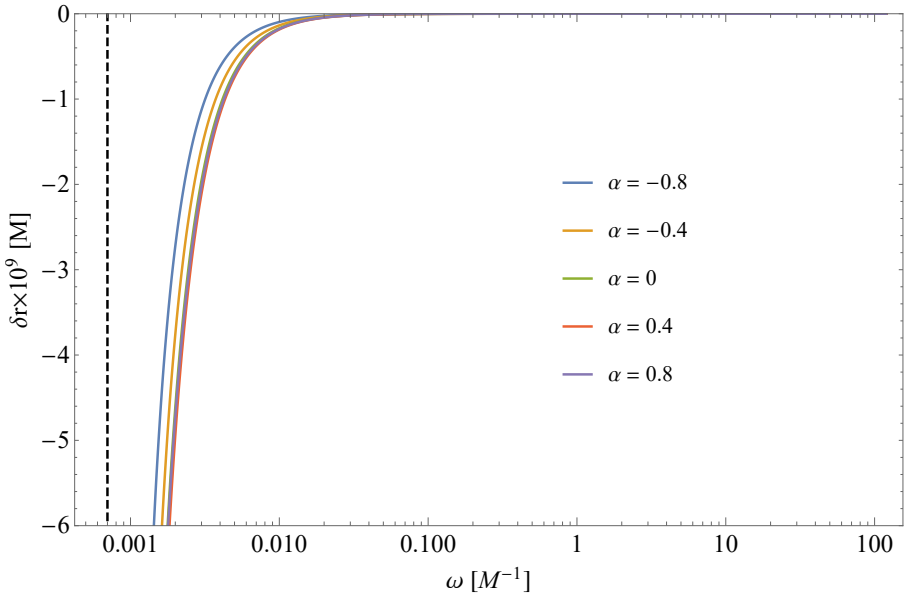

Figure 3.2: Newtonian dumbbell shifts are always negative and $\lim_{\omega\to\infty} \delta r = 0$ for any α. The dashed line is the limiting frequency corresponding to the free-fall time to the center.

If there were no effect, the shift δr would vanish identically. This is not the case but we can see the dumbbell is not swimming and, instead, it is "drowning"—whatever it does, whatever the deformation function is, it ends up lower than the reference particle. We also notice the divergence in the low-frequency region which is due to the fact that the lower end of the dumbbell reaches the center where the equations of motion become singular with infinite forces and accelerations. We now ask what the situation is in general relativity—can we swim, can we gain "height" by performing cyclic deformations instead of just falling passively? The answer is presented in Figure 3.3, which is one of the main results of our paper [43].

The situation has changed dramatically: for $\alpha < 0$ the dumbbell now falls more slowly than a point mass and so, in effect, it swims. The swimming only occurs for a certain range of frequencies but if it does then there is a plateau where the shift stays nearly constant. So far, these results are in agreement with [39]. We succeeded in extending the range of frequencies to both extremes where we can now observe divergences. The high-frequency divergence of the shift is simply due to the fact that we require the two endpoints to move ever faster until, for a critical frequency ω_c, they reach the velocity of light. There is no limiting speed in the Newtonian case so this phenomenon is only present in the relativistic treatment. This

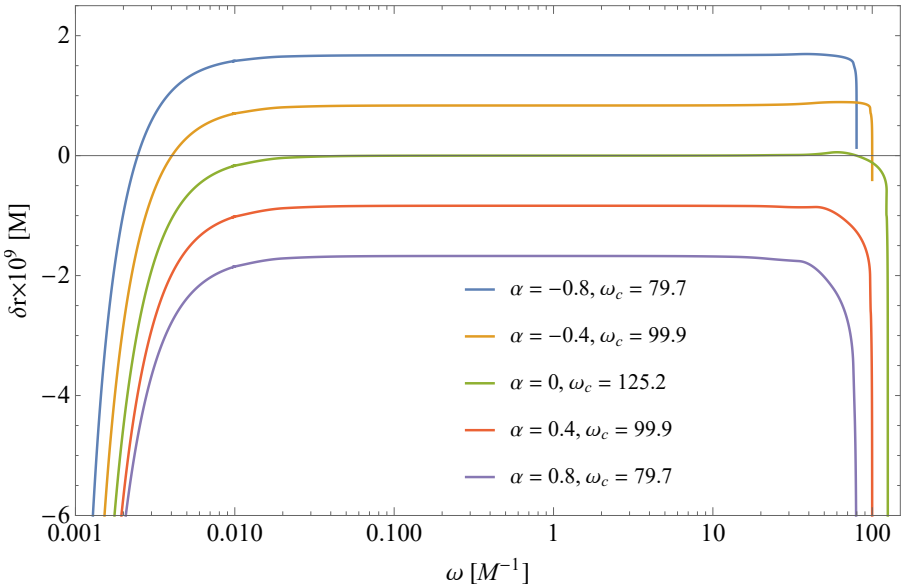

Figure 3.3: Relativistic shifts can be both negative and positive and they diverge for both high and low frequencies. The upper divergence frequency, ω_c, can be estimated analytically by assuming the dumbbell does not have time to move much before shrinking back to a point.

is a first indication that the Lagrangian we are using may be unphysical. Similarly to the Newtonian case, the lowest frequencies again signify that we are approaching a region where our coordinates cease describing the situation properly—this is the horizon of the black hole where Schwarzschild coordinates are inappropriate. In fact, the trajectory of the lower particle approximates a null path and our equations become singular again. There is another, purely geometrical, ingredient at play here: in Figure 3.3, we are only looking at endpoints $t = 1/\omega$ of evolution curves for varying frequencies but this means that for $\omega \to 0$ the derivative of the shift with respect to the frequency necessarily diverges

$$\frac{d}{d\omega}\delta r(\omega) = \frac{\partial}{\partial\omega}\delta r(t,\omega)\bigg|_{t=\frac{1}{\omega}} - \frac{\partial}{\partial t}\delta r(t,\omega)\bigg|_{t=\frac{1}{\omega}} \frac{1}{\omega^2}. \tag{3.4}$$

All the derivatives appearing here are finite according to our numerics so that for a finite ω the result is finite, too. However, if ω vanishes, the second term is unbounded and we get the divergence seen for low frequencies in our plot. This effect is at play in the Newtonian case of Figure 3.2 as well but here, we hit the center before this divergence occurs.

It is of interest that if we inspect the difference in the final dumbbell velocity after one full stroke minus the velocity of the reference point particle at the same time (negative values mean velocities directed towards the center) we always obtain a negative value, see Figure 3.4. Put differently, irrespective of the shift being positive or negative, the dumbbell always ends up falling faster towards the center than the point particle. This may come as a surprise for positive shifts but we must bear in mind that the difference in the velocities is only evaluated at the completion of the stroke and thus, throughout most of the fall, the differential velocity may well be positive which, integrated over time, yields a positive shift even for negative final velocities. The differential velocity inherited the two divergences from the shift function of plot Figure 3.3—both for the low and high oscillation frequencies.

Both divergences suggest the Lagrangian 3.1 yields unphysical results and must be abandoned. In hindsight, this is also obvious from the fact that the two particles know immediately

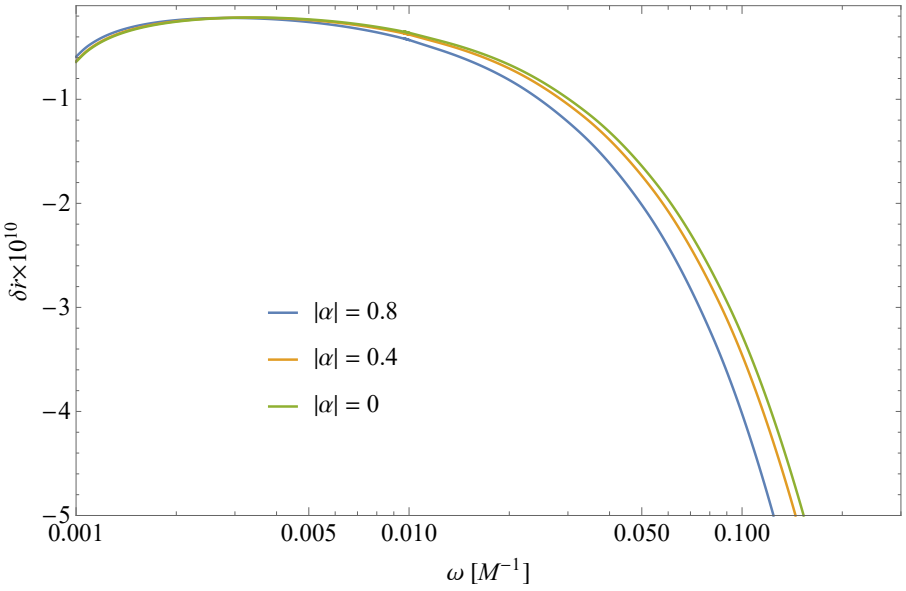

Figure 3.4: Differential velocity in the relativistic case. Its value is always negative, which indicates a greater velocity of the dumbbell towards the gravitational centre as compared to the reference particle. Unlike the shifts of Figure 3.3, the differential velocity is almost independent of the sign of α and decreases more rapidly for larger values of ω, hence the limited range of the plot. We again notice hints of divergence at both ends of the frequency spectrum.

about the position of their partner, which involves superluminal communication or action at a distance. So the question stands—can we build a better model? In the following section we shall show that this is indeed the case.

3.2 Discrete spring

In fact, we are trying to invent a general relativistic model of a spring that would only entail local interaction. We thus invoke interaction via exchange of point particles travelling along geodesics [44]. Since springs exhibit not only pressure but also tension—and tension is central to our dumbbell model that needs to contract—we need interaction particles that would push their targets in the direction opposite to the direction of motion of the interaction particles: we need interaction particles of a negative mass and thus with a 4-momentum pointing against their 4-velocity.

The oscillating dumbbell would be represented by an original single particle at a standstill at a given initial distance r_{ini} from the Schwarzschild black hole. Our experiment begins as the particle decays into two ordinary particles shooting out radially in opposite directions with a given initial coordinate velocity. The decay is governed by the conservation of 4-momentum that has only 2 non-vanishing components for the radial fall. Let us denote $\mu_i := m_i/M$, where the two products have masses m_i while the parent particle has a mass M. We can then write

$$\begin{aligned}\frac{\mathrm{d}t}{\mathrm{d}\tau} &= \mu_1\frac{\mathrm{d}t}{\mathrm{d}\tau_1} + \mu_2\frac{\mathrm{d}t}{\mathrm{d}\tau_2},\\ \frac{\mathrm{d}r}{\mathrm{d}\tau} &= \mu_1\frac{\mathrm{d}r}{\mathrm{d}\tau_1} + \mu_2\frac{\mathrm{d}r}{\mathrm{d}\tau_2},\end{aligned} \tag{3.5}$$

with the subscripts referring to the two product particles. The above relations and normalization of the three 4-velocities together with the initial velocity of the original particle determine the velocities of the outgoing particles. Instead of fixing the product masses and the mass of the decaying particle we can equivalently fix the velocities of the products. Following the decay, the two particles move along geodesics. After a proper time τ measured independently and locally by the two particles, they both decay again into an ordinary particle and an exchange particle of a negative mass, which flies towards the other end of the dumbbell, pulling their decay partner a bit along. As the exchange particles hit their targets they merge with them to produce ordinary particles approaching each other until they finally fuse to form the final product—a single particle closer to the black hole. We now measure the difference between the final position and that of a single reference particle falling with the same initial conditions. We define the frequency of the process to be the inverse of the total time it takes to come back to a single point. See Figure 3.5 for a spacetime-diagram sketch of the discrete spring model.

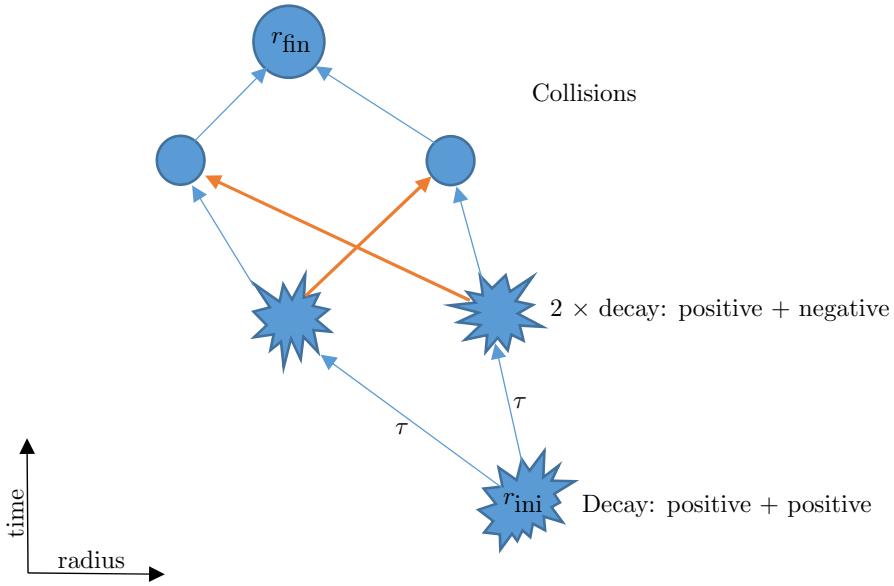

Figure 3.5: A schematic diagram of the discrete spring model with time pointing upwards and the black hole located to the left. The original particle is dropped from rest at an initial distance r_{ini} from the center and it is shown at the bottom of the diagram as it decays into two intermediate particles flying in opposite directions for an interval of their proper time τ after which they decay again, both releasing a standard particle with a positive mass and an interaction particle with a negative mass. The interaction particles fly in the direction opposite to their mother particles, hitting the other end of the "spring" after some time and bringing it back to finally collide and merge to produce the final standard particle at a distance r_{fin}. Trajectories of positive-mass particles are shown using blue arrows, while negative-mass particles have orange arrows. Decays are depicted as stars, collisions as circles. Between their encounters, all particles move on geodesics.

We now just mention in passing the theory of extended bodies in general relativity—Dixon's approach [45, 46, 47]. It describes the evolution of objects which have a stress-energy tensor satisfying the standard conservation laws $T^{\alpha}_{\alpha} = 0$. The theory uses an expansion in terms of multipole moments of the stress-energy tensor and gives evolution equations for them. One of its results relevant for us is that in maximally symmetric spacetimes—that is, the Minkowski,

de Sitter, and anti de Sitter spacetimes—the center of mass of such bodies, which can be defined in this case, moves along a geodesic. It follows then that our dumbbell should see no shift after a full stroke cycle as compared to a simple point mass. However, if we integrate the equations of motion following from the Lagrangian 3.1 in these spacetimes we still get a non-vanishing shift. This further confirms our previous conclusion that the Lagrangian is unphysical and misleading and we were right to abandon it.

We now run the same de Sitter/anti de Sitter test for our discrete spring model consisting of geodetic particles, which necessarily satisfies the conservation laws. The main advantage of the model consists in the fact that, in principle, it admits an analytical solution. However, it turns out that a numerical approach is much faster and we thus simply solve the geodesic equations numerically to find where and when the collisions between our particles occur. When choosing the parameters of our system—the time to decay, τ, and the velocities of the initial decay products—we need to make sure all the particles stay within the null cone. The results are presented in Figure 3.6. Notice the difference in the order of magnitude of our results from those of Figure 3.3. Allowing for numerical errors, we conclude that the shift vanishes as expected and, indeed, no swimming occurs here. This verifies the viability of our model and we can now proceed to drop the discrete spring into a Schwarzschild black hole to see whether it can still swim like the dumbbell apparently did.

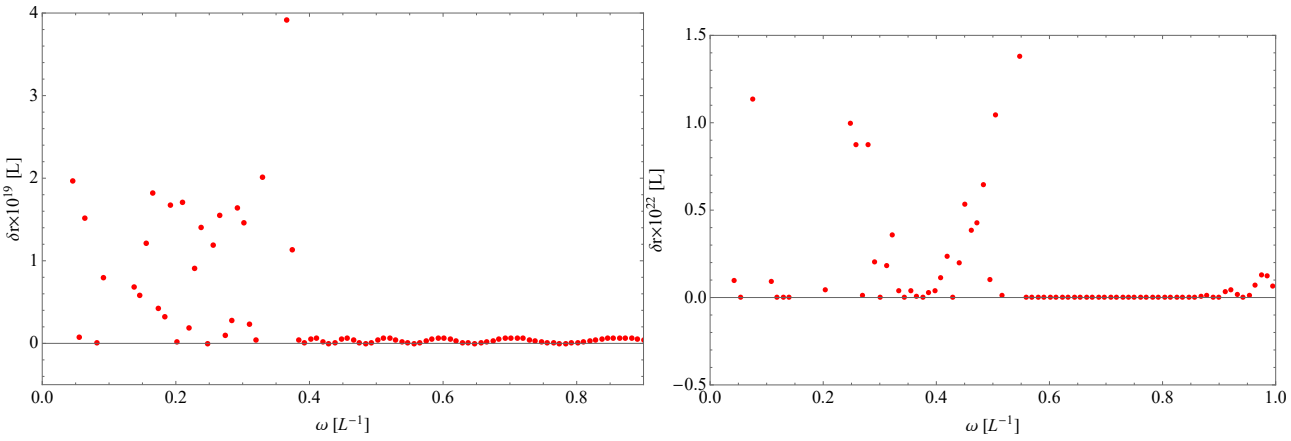

Figure 3.6: Shift of the discrete spring model compared to a point mass in de Sitter (left) and anti de Sitter (right) spacetimes with $L = 1/\sqrt{|\Lambda|}$. The shifts are 10 orders of magnitude smaller than in the Schwarzschild case and appear to be random.

Therefore, we now return to the Schwarzschild spacetime and drop our system down the black hole. We choose such parameters that the first two decay products first fly apart for a relatively long time before decaying again with the messenger particles flying quickly back and hitting the standard particles to bring them back together in a relatively short time. This corresponds to $\alpha < 0$ for the unphysical dumbbell of Figure 3.3, which was supposed to swim, i.e., fall more slowly than a reference particle. Can we see any effect here?

Yes, as Figure 3.7 suggests, we can indeed. Unfortunately for all our hopes of swimming, the shift is negative for all values of the frequency parameter, ω. In fact, this is much more in keeping with the Newtonian case of 3.2, which should result from the relativistic case in the Newtonian limit. To conclude, using a discrete spring model based on subluminal interaction communicated by geodesic messenger particles, we can only drown compared to a point particle—it is better not to move at all. Whatever our deformation, we fall faster.

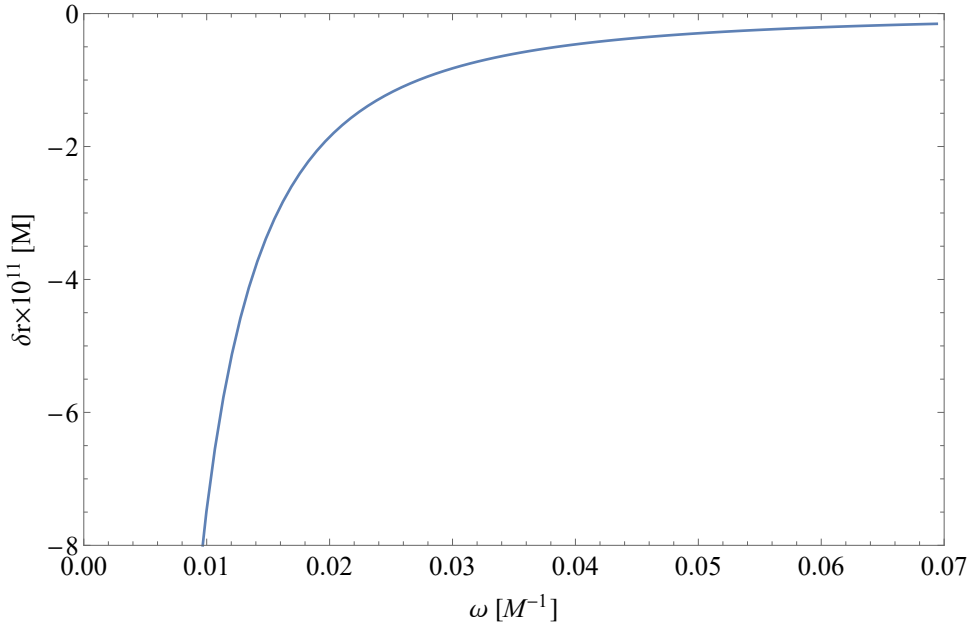

Figure 3.7: Relativistic shifts for the discrete spring model compared to a point mass in the field of a Schwarzschild black hole. The situation corresponds to $\alpha < 0$ but the shifts are only negative. The initial conditions are the same as for Figure 3.3.

In this chapter, we have shown that a dumbbell model with a prescribed and fixed deformation as a function of time is unphysical. We have proposed a simple physical model exhibiting cyclic deformations and based on geodesic motion and exchange of momentum between particles as they decay and merge. As a result, the shifts with respect to a reference point mass are always negative for radial paths in the Schwarzschild geometry unlike those purported for the dumbbell glider. Therefore, we must conclude that there is no swimming in the studied situations. Can we still save the day? In fact, there is a much stronger effect for a perpendicular oscillator, present already in the Newtonian case and resulting from the centrifugal force. One of our goals is to look at this case but it is not quite clear how to achieve this with the discrete model. Perhaps one could look at a simpler spacetime of the cosmic string [48, 6, 11] instead, which is locally Minkowskian and geodesics are thus just straight lines yielding analytical solutions for motion. Another possible case follows from the observation that the discrete spring is passive, meaning it just "flows" with the spacetime curvature. But swimmers in fact use internal energy to turn it into motion—we need an active swimmer. To improve our discrete spring model, we can use rockets instead of geodesic particles and see how that changes the outcome. This should be fairly easy to accomplish given our current setup but, on the other hand, one then loses the concept of a reactionless drive. Finally, another possible model of cyclic motion is that of a finite cosmic string with its endpoints attached to two massive particles. The tension in the string makes the two particles accelerate and the entire system, in fact, is an exact solution of Einstein equations [49, 50, 51] unlike our test models above. It would be of interest to see how it affects our no-swimming results above. So, perhaps, there is still hope.

4 Higher dimensions

When formulating his equations of general relativity, Einstein originally envisaged the spacetime to have 3 dimensions of space plus 1 of time and yet, the resulting formulation does not need to mention the number of dimensions we work in. We can thus easily generalize the theory to higher dimensions by simply allowing the indices appearing in the tensor equations to take on values beyond 0 to 3. In fact, this has actually been a very rich and rewarding field since the very beginning of general relativity, with one of the first attempts at uniting gravity and electromagnetism in 5D by Kaluza [52] already in 1921. This approach has blossomed to 11 spacetime dimensions required by consistency of the present-day M-theory [53]. In this thesis, we have also used a particular higher-dimensional solution of Einstein–Maxwell equations in Chapter 2 to subsequently reduce it back to 4D.

Here, we shall mention our work on a special family of solutions, the Robinson–Trautman class of spacetimes [54, 55], see also [11, 6], which admit a non-twisting, non-shearing but expanding family of null geodesics. This invariant definition is based on the optical properties of null geodesic congruences in higher-dimensional spacetimes as investigated in [56, 57] (for a review, refer to [58]). Though seemingly simple, the above assumption strongly restricts the admissible form of the metric tensor so that even without using Einstein equations we are able to infer the general form of the corresponding metric

$$\mathrm{d}s^2 = g_{ij}\left(\mathrm{d}x^i + g^{ri}\mathrm{d}u\right)\left(\mathrm{d}x^j + g^{rj}\mathrm{d}u\right) - 2\,\mathrm{d}u\mathrm{d}r - g^{rr}\mathrm{d}u^2, \tag{4.1}$$

in coordinates adapted to the null congruence $\boldsymbol{k}$ defining the RT family [59] where the Latin indices denote the $D-2$ transverse spatial dimensions, u =const are null hypersurfaces normal to $\boldsymbol{k}$, and r is the affine parameter along the geodesics generated by $\boldsymbol{k}=\partial_r$. The above requirements on the optical scalars of the metric reduce the metric coefficients even further but there is still some gauge freedom left to simplify the metric once we define the matter content of the spacetime. As the final step after these purely geometric considerations, we thus now impose physics in the form of Einstein equations with a particular form of the gravitating matter. In our case, we were interested in Maxwell fields aligned with the master null congruence so that $\boldsymbol{k}$ is an eigenvector of the electromagnetic field

$$F_{\alpha\beta}k^\beta = \mathcal{N}\,k_\alpha, \tag{4.2}$$

demanding that Einstein–Maxwell equations be satisfied throughout the spacetime. Since we are dealing with a spacetime of a general dimension $D>3$, we need to calculate all Einstein and Maxwell tensorial components by hand and plug them into our equations. Until recently there has been no computer algebra system that would not require a particular number of dimensions to be fixed. Today there is *xAct* [60], which is capable of performing some calculations of this type.

After considerable algebraic manipulations, we were able to show how the metric functions are restricted as regards their dependance on the coordinates. In particular, we found that the metric must be of the following simpler form

$$\mathrm{d}s^2 = r^2\,h_{ij}(x)\,\mathrm{d}x^i\mathrm{d}x^j - 2\,\mathrm{d}u\mathrm{d}r - 2H(r)\,\mathrm{d}u^2. \tag{4.3}$$

The function $2H$ and the Maxwell field $\boldsymbol{F}$ depend on the dimension: for an even dimension $4<D\neq 6$ we obtained

$$2H = K - \frac{2\Lambda}{(D-2)(D-1)}\,r^2 - \frac{\mu}{r^{D-3}} + \frac{2Q^2}{(D-2)(D-3)}\frac{1}{r^{2(D-3)}} - \frac{F^2}{(D-2)(D-5)}\frac{1}{r^2}\,, \tag{4.4}$$

and

$$\boldsymbol{F} = \frac{Q}{r^{D-2}} \mathrm{d}r \wedge \mathrm{d}u + \tfrac{1}{2} F_{ij}(x)\, \mathrm{d}x^i \wedge \mathrm{d}x^j, \tag{4.5}$$

where $K = \pm 1, 0$, and μ, Q, F are constants denoting the mass and electric and magnetic charges of the spacetime. As always, Λ is the cosmological constant, which determines the character of the asymptotic region. Inspecting the Ricci scalar, we conclude there is a curvature singularity located at the origin of coordinates and it is generally hidden behind an event horizon. The transverse $(D-2)$-dimensional manifold is a Riemannian Einstein space, and if it is compact then these solutions can be interpreted as a black hole.

In odd dimensions, we find $F = 0$ identically, otherwise the form of the solution is the same. With a vanishing magnetic field, the solutions are a generalization of the Reissner–Nordström-(anti) de Sitter spacetimes to higher dimensions. The $D = 6$ case is surprisingly complicated and we have not completed its full analysis yet. These results are the main outcome of our paper [61]. In a follow-up paper [62] we then investigated the natural counterpart of the Robinson–Trautman class of spacetimes—the Kundt family, which only differs in the fact that the master congruence is non-expanding. We again found all admissible forms of the metric and electromagnetic fields and identified interesting subclasses of these solutions, such as pp-waves, VSI and CSI spacetimes, and gyratons.

In our final paper [63], we returned to the higher-dimensional Robinson–Trautman class but admitted an aligned p-form generalization of the Maxwell field. The solutions depend strongly on both p and the dimension D. In odd dimensions the solutions represent static black holes with electric and magnetic fields. There are more options in even dimensions and, for instance, if $2p = D$ there are non-static solutions describing black holes immersed in electromagnetic radiation. The above observation on the very different properties of even and odd dimensions despite identical assumptions on both physics and geometry of the spacetime appears to be quite general. Let us conclude by noting that the standard four-dimensional family of spacetimes is richer than higher-dimensional solutions that—perhaps surprisingly—constrain the admissible form of the metric more strictly. In a way, four dimensions are very special indeed. The topic of black holes in higher dimensions is a lively field [64] and the approach consisting of first demanding some geometric properties of the metric and then imposing physics in the form of Einstein equations has yielded new insights in the hot topic of higher-dimensional spacetimes.

5 Cylinders

As mentioned in the Introduction and also evidenced by Chapter 1, cylindrically symmetric systems are of interest in general relativity from the point of view of simplifying Einstein equations while still providing a wide class of solutions relevant for physics [65]. It should also be noted that one of the most important topics in general relativity—generation and propagation of gravitational waves—also singles out cylindrical symmetry as a suitable test-bed for studying various effects due to the interplay between collapsing matter and gravitational radiation [66]. Indeed, the astronomically most natural assumption of spherical symmetry for a collapsing object of a finite dimension and thus with a vacuum field outside leads through the Birkhoff's theorem [67, 68] to the conclusion that the exterior gravitational field is static, that is, non-radiative. Cylindrical symmetry is the next best thing one can use to reduce the equations and achieve an analytical solution [69]. In order to understand these highly complicated and dynamic solutions it is best to start out by studying their static counterparts, either vacuum [70] or involving electromagnetic [71] or even matter fields [72].

Apart from the paper [7] already mentioned in Chapter 1, we also published a paper [73] on application of the Israel formalism [74] describing the fields of planar matter sources resulting from the cutting and pasting method familiar from the classical Maxwell theory. In essence, one removes a part of a given spacetime and identifies the remaining parts along a hypersurface of a dimension lower by 1, or one identifies two arbitrary spacetimes along a selected hypersurface. Just like for the electromagnetic field where the precondition is that the parallel component of the electric field and the perpendicular component of the magnetic field be continuous across the boundary, in general relativity we must demand that the 3D metric tensor induced on the boundary hypersurface be the same from both sides. This is a very useful approach, generalizable also to non-vacuum fields [75] and often enabling us to remove singularities of a particular gravitational field by simply dropping the regions where they occur and replacing them with planar distributions of matter and fields. In [73] we first studied spherically symmetric, dynamically evolving vacuum bubbles glued inside-out on themselves and forming thus the entirety of the universe, and then we focused on cylindrically symmetric fields of the so-called cosmic strings [48]. We showed that regardless of a particular model of sheet sources for the cosmic string, the limiting process where we restrict the perpendicular dimension of the model always yields the same result.

In [76], we investigated the gravitational fields of infinite cylinders of a finite radius and made of perfect fluid. We assumed the field outside is described by the Levi-Civita solution [8]. It is of interest that there is no analytical solution of this class unlike in the spherically symmetric situation where we have the interior Schwarzschild solution [77]. This meant that we needed to resort to numerical calculations, however, we succeeded in proving the existence and uniqueness of the solutions within the entire domain without much restricting the equation of state of the constituent fluid. One of the basic questions one asks when solving an analogous problem in spherical symmetry—that is, when one constructs a model of a star—is the resulting object finite in the radial direction? We provided an answer for cylindrical symmetry and showed that if the fluid has a non-zero density even when its pressure vanishes then the radius of the cylinder is finite. We were even able to find an analytical solution if the fluid is incompressible and its gravitational field is weak. We discussed in detail the geometric properties of the resulting spacetimes and the physical characteristics of the cylinders, such as their conicity and linear mass.

Our paper [78] deals with a generalization of the Levi-Civita spacetime to include a non-vanishing cosmological constant, the Linet–Tian spacetime [79, 80]. In particular, we again used the Israel formalism to find non-singular sheet sources of the field and described their characteristics, we further found how the Linet–Tian solution is related to the 4D black-string solutions [81]. We confirmed our previous estimate on the upper limit of linear mass density of these sources, $M_1 \leq 1/4$. We further noted that to the lowest order in the cylindrical radial infinity, the solution with $\Lambda < 0$ is analogous to the Schwarzschild anti de Sitter spacetime, highlighting thus its role similar to spatially bounded systems with a vanishing cosmological constant. The papers [76, 78] are an example of a general effort to find physically acceptable, that is, non singular sources of vacuum spacetimes which are often due to a point-like singularity—think of the Schwarzschild solution—or line-like singularity, which is the case of the Levi-Civita and Linet–Tian spacetimes.

Although exact cylindrical symmetry is obviously not achieved in Nature, this assumption still provides us with many interesting solutions within the framework of general relativity and the field is very active today. Some of the current topics include gravitational lensing by cosmic strings [82], cylindrical wormholes [83], fields of rotating cylinders and non-vacuum solutions [84, 85], and propagation of gravitational waves [86].

Let me conclude this chapter on a humorous note by noting that my very first publication—a conference proceedings contribution from 1996 [87]—also concerned a cylindrically symmetric system although it had no relation to the general theory of relativity whatsoever. The paper resulted from my cooperation with Prof. V.M. Kenkre (University of New Mexico, USA) on analytical calculations of temperature distribution in a cylindrical vessel of liquid helium near the critical temperature T_λ.

Bibliography

[1] Bonnor W B 1954 Static magnetic fields in general relativity *Proceedings of the Physical Society. Section A* **67** 225–232 URL https://doi.org/10.1088%2F0370-1298%2F67%2F3%2F305

[2] Melvin M 1964 Pure magnetic and electric geons *Physics Letters* **8** 65–68 ISSN 0031-9163 URL http://www.sciencedirect.com/science/article/pii/0031916364908017

[3] Wheeler J A 1955 Geons *Phys. Rev.* **97**(2) 511–536 URL https://link.aps.org/doi/10.1103/PhysRev.97.511

[4] Brill D R and Hartle J B 1964 Method of the self-consistent field in general relativity and its application to the gravitational geon *Phys. Rev.* **135**(1B) B271–B278 URL https://link.aps.org/doi/10.1103/PhysRev.135.B271

[5] Anderson P R and Brill D R 1997 Gravitational geons revisited *Phys. Rev. D* **56**(8) 4824–4833 URL https://link.aps.org/doi/10.1103/PhysRevD.56.4824

[6] Griffiths J B and Podolský J 2009 *Exact Space-Times in Einstein's General Relativity* Cambridge Monographs on Mathematical Physics (Cambridge: Cambridge University Press)

[7] Žofka M and Langer J 2005 Relativistic solenoids *Czechoslovak Journal of Physics* **55** 157–165 ISSN 1572-9486 URL https://doi.org/10.1007/s10582-005-0027-9

[8] Levi-Civita T 1919 ds2 einsteiniani in campi newtoniani. IX: L'analogo del potenziale logaritmico *Atti della Reale Accademia dei Lincei* **28** 101–109 URL http://villafarnesina.it/pubblicazioni/rendicontiFMN/rol/pdf/S5V28T1A1919P101_109.pdf

[9] Einstein A 1917 Kosmologische Betrachtungen zur allgemeinen Relativitätstheorie *Sitzungsberichte der Königlich Preußischen Akademie der Wissenschaften (Berlin)* 142–152 URL http://articles.adsabs.harvard.edu/cgi-bin/get_file?pdfs/SPAW./1917/1917SPAW.....142E.pdf

[10] Planck Collaboration 2018 Planck 2018 results. VI. Cosmological parameters (*Preprint* arXiv:https://arxiv.org/abs/1807.06209v2)

[11] Stephani H, Kramer D, MacCallum M A, Hoenselaers C and Herlt E 2003 *Exact solutions of Einstein's field equations* 2nd ed Cambridge Monographs on Mathematical Physics (Cambridge: Cambridge University Press) ISBN 9780521467025, 0521467020, 9780511059179, 9780521467025 URL https://www.cambridge.org/core/books/exact-solutions-of-einsteins-field-equations/11CF6CFCC10CC62B9B299F08C32C37A6

[12] Smolić I 2015 Symmetry inheritance of scalar fields *Classical and Quantum Gravity* **32** 145010 URL https://doi.org/10.1088%2F0264-9381%2F32%2F14%2F145010

[13] MacCallum M A H and Santos N O 1998 Stationary and static cylindrically symmetric Einstein spaces of the Lewis form *Classical and Quantum Gravity* **15** 1627–1636 URL https://doi.org/10.1088%2F0264-9381%2F15%2F6%2F017

[14] Plebański J F and Hacyan S 1979 Some exceptional electrovac type D metrics with cosmological constant *Journal of Mathematical Physics* **20** 1004–1010 URL https://doi.org/10.1063/1.524174

[15] Žofka M 2019 Bonnor–Melvin universe with a cosmological constant *Phys. Rev. D* **99** 044058 URL https://link.aps.org/doi/10.1103/PhysRevD.99.044058

[16] Pravda V and Pravdová A 2000 Boost-rotation symmetric spacetimes – Review *Czechoslovak Journal of Physics* **50** 333–375 ISSN 0011-4626 URL http://dx.doi.org/10.1023/A:1022862309863

[17] Carot J and da Costa J 1993 On the geometry of warped spacetimes *Classical and Quantum Gravity* **10** 461–482 URL https://doi.org/10.1088%2F0264-9381%2F10%2F3%2F007

[18] Veselý J and Žofka M 2019 Cosmological magnetic field: The boost-symmetric case *Phys. Rev. D* **100**(4) 044059 URL https://link.aps.org/doi/10.1103/PhysRevD.100.044059

[19] Majumdar S D 1947 A class of exact solutions of Einstein's field equations *Phys. Rev.* **72**(5) 390–398 URL https://link.aps.org/doi/10.1103/PhysRev.72.390

[20] Papapetrou A 1945 A static solution of the equations of the gravitational field for an arbitary charge-distribution *Proceedings of the Royal Irish Academy. Section A: Mathematical and Physical Sciences* **51** 191–204 ISSN 00358975 URL http://www.jstor.org/stable/20488481

[21] Hartle J B and Hawking S W 1972 Solutions of the Einstein–Maxwell equations with many black holes *Comm. Math. Phys.* **26** 87–101 URL https://projecteuclid.org:443/euclid.cmp/1103858037

[22] Ryzner J and Žofka M 2015 Electrogeodesics in the di-hole Majumdar–Papapetrou spacetime *Classical and Quantum Gravity* **32** 205010 URL https://doi.org/10.1088%2F0264-9381%2F32%2F20%2F205010

[23] Ryzner J and Žofka M 2016 Extremally charged line *Classical and Quantum Gravity* **33** 245005 URL https://doi.org/10.1088%2F0264-9381%2F33%2F24%2F245005

[24] Havil J 2003 *Gamma: Exploring Euler's Constant* (Princeton University Press) ISBN 9780691141336 URL http://www.jstor.org/stable/j.ctt7sd75

[25] Ryzner J and Žofka M 2019 Crystal spacetimes with discrete translational symmetry *Einstein Equations: Physical and Mathematical Aspects of General Relativity: Domoschool 2018* ed Cacciatori S, Güneysu B and Pigola S (Cham: Springer International Publishing) pp 289–312 ISBN 978-3-030-18061-4 URL https://doi.org/10.1007/978-3-030-18061-4_10

[26] Amsel A J, Horowitz G T, Marolf D and Roberts M M 2010 Uniqueness of extremal Kerr and Kerr–Newman black holes *Phys. Rev. D* **81**(2) 024033 URL https://link.aps.org/doi/10.1103/PhysRevD.81.024033

[27] Lemos J P S and Zanchin V T 2005 Class of exact solutions of Einstein's field equations in higher dimensional spacetimes, $d \geq 4$: Majumdar–Papapetrou solutions *Phys. Rev. D* **71**(12) 124021 URL https://link.aps.org/doi/10.1103/PhysRevD.71.124021

[28] Frolov V P and Zelnikov A 2012 Scalar and electromagnetic fields of static sources in higher dimensional Majumdar–Papapetrou spacetimes *Phys. Rev. D* **85**(6) 064032 URL https://link.aps.org/doi/10.1103/PhysRevD.85.064032

[29] Myers R C 1987 Higher-dimensional black holes in compactified space-times *Phys. Rev. D* **35**(2) 455–466 URL https://link.aps.org/doi/10.1103/PhysRevD.35.455

[30] Wirkus S, Rand R and Ruina A 1998 How to pump a swing *The College Mathematics Journal* **29** 266–275 URL https://doi.org/10.1080/07468342.1998.11973953

[31] Rica da Silva A J and Lemos J P S 2008 Binary collisions and the slingshot effect *Celestial Mechanics and Dynamical Astronomy* **100** 191–208 ISSN 1572-9478 URL https://doi.org/10.1007/s10569-007-9114-5

[32] Guéron E, Maia C A S and Matsas G E A 2006 Swimming versus swinging effects in spacetime *Phys. Rev. D* **73**(2) 024020 URL https://link.aps.org/doi/10.1103/PhysRevD.73.024020

[33] Murray C D and Dermott S F 2000 *Solar System Dynamics* (Cambridge: Cambridge University Press)

[34] Yamagiwa Y, Nohmi M, Aoki Y, Momonoi Y, Nanba H, Aiga M, Kumao T and Watahiki M 2017 Space experiments on basic technologies for a space elevator using microsatellites *Acta Astronautica* **138** 570–578 ISSN 0094-5765 URL http://www.sciencedirect.com/science/article/pii/S0094576516307457

[35] Burov A A and Kosenko I I 2015 Planar oscillations of a dumb-bell of a variable length in a central field of Newtonian attraction. Exact approach *International Journal of Non-Linear Mechanics* **72** 1–5 ISSN 0020-7462 URL http://www.sciencedirect.com/science/article/pii/S0020746215000293

[36] Longo M J 2004 Swimming in Newtonian space-time: Orbital changes by cyclic changes in body shape *American Journal of Physics* **72** 1312–1315 URL https://doi.org/10.1119/1.1773576

[37] Cartmell M and McKenzie D 2008 A review of space tether research *Progress in Aerospace Sciences* **44** 1–21 ISSN 0376-0421 URL http://www.sciencedirect.com/science/article/pii/S0376042107000656

[38] Johnson L, Bilén S G, Gilchrist B E and Krause L H 2017 Tethers in space *Acta Astronautica* **138** 502 ISSN 0094-5765 URL http://www.sciencedirect.com/science/article/pii/S0094576517309463

[39] Guéron E and Mosna R A 2007 Relativistic glider *Phys. Rev. D* **75**(8) 081501 URL https://link.aps.org/doi/10.1103/PhysRevD.75.081501

[40] Bloch A M, Leonard N E and Marsden J E 1997 Stabilization of mechanical systems using controlled lagrangians *Proceedings of the 36th IEEE Conference on Decision and Control* vol 3 pp 2356–2361 vol.3 ISSN 0191-2216 URL https://doi.org/10.1109/CDC.1997.657135

[41] Shiriaev A S, Freidovich L B and Spong M W 2013 A remark on controlled lagrangian approach *European Journal of Control* **19** 438–444 ISSN 0947-3580 URL http://www.sciencedirect.com/science/article/pii/S0947358013001593

[42] Puiggalí M F and Mestdag T 2016 The inverse problem of the calculus of variations and the stabilization of controlled lagrangian systems *SIAM Journal on Control and Optimization* **54** 3297–3318 URL https://doi.org/10.1137/16M1060091

[43] Veselý V and Žofka M 2019 How to glide in Schwarzschild spacetime *Classical and Quantum Gravity* **36** 075011 URL https://doi.org/10.1088%2F1361-6382%2Fab0976

[44] Slezák D 2018 *Model of relativistic spinning system* Bachelor's thesis Charles University URL https://is.cuni.cz/webapps/zzp/detail/156531/

[45] Dixon W G 1970 Dynamics of Extended Bodies in General Relativity. I. Momentum and Angular Momentum *Proceedings of the Royal Society of London. Series A, Mathematical and Physical Sciences* **314** 499–527 ISSN 00804630 URL http://www.jstor.org/stable/2416466

[46] Dixon W G 1970 Dynamics of Extended Bodies in General Relativity. II. Moments of the Charge-Current Vector *Proceedings of the Royal Society of London. Series A, Mathematical and Physical Sciences* **319** 509–547 ISSN 00804630 URL http://www.jstor.org/stable/77735

[47] Dixon W G 1974 Dynamics of Extended Bodies in General Relativity. III. Equations of Motion *Philosophical Transactions of the Royal Society of London. Series A, Mathematical and Physical Sciences* **277** 59–119 ISSN 00804614 URL http://www.jstor.org/stable/74364

[48] Vilenkin A 1981 Gravitational field of vacuum domain walls and strings *Phys. Rev. D* **23**(4) 852–857 URL https://link.aps.org/doi/10.1103/PhysRevD.23.852

[49] Griffiths J B, Krtouš P and Podolský J 2006 Interpreting the C-metric *Classical and Quantum Gravity* **23** 6745–6766 URL https://doi.org/10.1088%2F0264-9381%2F23%2F23%2F008

[50] Kinnersley W and Walker M 1970 Uniformly accelerating charged mass in general relativity *Phys. Rev. D* **2**(8) 1359–1370 URL https://link.aps.org/doi/10.1103/PhysRevD.2.1359

[51] Bonnor W B 1983 The sources of the vacuum C-metric *General Relativity and Gravitation* **15** 535–551 ISSN 1572-9532 URL https://doi.org/10.1007/BF00759569

[52] Kaluza T 1921 Zum Unitätsproblem der Physik *Sitzungsberichte der Königlich Preußischen Akademie der Wissenschaften (Berlin)* 966–972 URL http://inspirehep.net/record/14621/files/kaluza.pdf

[53] Miemiec A and Schnakenburg I 2006 Basics of M-theory *Fortschritte der Physik* **54** 5–72 URL https://onlinelibrary.wiley.com/doi/abs/10.1002/prop.200510256

[54] Robinson I and Trautman A 1960 Spherical gravitational waves *Phys. Rev. Lett.* **4**(8) 431–432 URL https://link.aps.org/doi/10.1103/PhysRevLett.4.431

[55] Robinson I and Trautman A 1962 Some spherical gravitational waves in general relativity *Proceedings of the Royal Society of London. Series A, Mathematical and Physical Sciences* **265** 463–473 ISSN 00804630 URL http://www.jstor.org/stable/2414275

[56] Frolov V and Stojković D 2003 Particle and light motion in a space-time of a five-dimensional rotating black hole *Phys. Rev. D* **68**(6) 064011 URL https://link.aps.org/doi/10.1103/PhysRevD.68.064011

[57] Pravda V, Pravdová A, Coley A and Milson R 2004 Bianchi identities in higher dimensions *Classical and Quantum Gravity* **21** 2873–2897 URL https://doi.org/10.1088%2F0264-9381%2F21%2F12%2F007

[58] Coley A 2008 Classification of the Weyl tensor in higher dimensions and applications *Classical and Quantum Gravity* **25** 033001 URL https://doi.org/10.1088%2F0264-9381%2F25%2F3%2F033001

[59] Podolský J and Ortaggio M 2006 Robinson–Trautman spacetimes in higher dimensions *Classical and Quantum Gravity* **23** 5785–5797 URL https://doi.org/10.1088%2F0264-9381%2F23%2F20%2F002

[60] Martín-García J M 2002-2018 xAct: Efficient tensor computer algebra for the Wolfram Language URL http://www.xAct.es

[61] Ortaggio M, Podolský J and Žofka M 2008 Robinson–Trautman spacetimes with an electromagnetic field in higher dimensions *Classical and Quantum Gravity* **25** 025006 URL https://doi.org/10.1088%2F0264-9381%2F25%2F2%2F025006

[62] Podolský J and Žofka M 2009 General Kundt spacetimes in higher dimensions *Classical and Quantum Gravity* **26** 105008 URL https://doi.org/10.1088%2F0264-9381%2F26%2F10%2F105008

[63] Ortaggio M, Podolský J and Žofka M 2015 Static and radiating p-form black holes in the higher dimensional Robinson–Trautman class *Journal of High Energy Physics* **2015** 45 ISSN 1029-8479 URL https://doi.org/10.1007/JHEP02(2015)045

[64] Kleihaus B and Kunz J 2016 Black holes in higher dimensions (black strings and black rings) (*Preprint* arXiv:https://arxiv.org/abs/1603.07267)

[65] Bronnikov K, Santos N and Wang A 2019 Cylindrical systems in general relativity (*Preprint* arXiv:https://arxiv.org/abs/1901.06561v2)

[66] García-Parrado A and Mena F C 2018 Gravitational radiation and the evolution of gravitational collapse in cylindrical symmetry (*Preprint* arXiv: https://arxiv.org/abs/1811.10303v1)

[67] Jebsen J T 2005 On the general spherically symmetric solutions of Einstein's gravitational equations in vacuo *General Relativity and Gravitation* **37** 2253–2259 ISSN 1572-9532 URL https://doi.org/10.1007/s10714-005-0168-y

[68] Birkhoff G D and Langer R E 1923 *Relativity and modern physics* (Cambridge: Harvard University Press)

[69] Nakao K and Morisawa Y 2004 High speed dynamics of collapsing cylindrical dust fluid *Classical and Quantum Gravity* **21** 2101–2113 URL https://doi.org/10.1088%2F0264-9381%2F21%2F8%2F013

[70] Wang A Z, da Silva M F A and Santos N O 1997 On parameters of the Levi-Civita solution *Classical and Quantum Gravity* **14** 2417–2423 URL https://doi.org/10.1088%2F0264-9381%2F14%2F8%2F033

[71] Miguelote A Y, da Silva M F A, Wang A Z and Santos N O 2001 Levi-Civita solutions coupled with electromagnetic fields *Classical and Quantum Gravity* **18** 4569–4588 URL https://doi.org/10.1088%2F0264-9381%2F18%2F21%2F312

[72] Brito I, Carot J, Mena F C and Vaz E G L R 2012 Cylindrically symmetric static solutions of the Einstein field equations for elastic matter *Journal of Mathematical Physics* **53** 122504 URL https://doi.org/10.1063/1.4769223

[73] Langer J and Žofka M 2002 Nearly everywhere flat spaces *Czechoslovak Journal of Physics* **52** 669–677 ISSN 1572-9486 URL https://doi.org/10.1023/A:1015578527559

[74] Israel W 1966 Singular hypersurfaces and thin shells in general relativity *Nuovo Cim. B* **44** 1–14 ISSN 1826-9877 [Erratum: 1967 Nuovo Cim. B 48 463] URL https://doi.org/10.1007/BF02710419

[75] Kuchař K 1968 Charged shells in general relativity and their gravitational collapse *Czechoslovak Journal of Physics B* **18** 435–463 ISSN 1572-9486 URL https://doi.org/10.1007/BF01698208

[76] Bičák J, Ledvinka T, Schmidt B G and Žofka M 2004 Static fluid cylinders and their fields: global solutions *Classical and Quantum Gravity* **21** 1583–1608 URL https://doi.org/10.1088%2F0264-9381%2F21%2F6%2F019

[77] Schwarzschild K 1916 Über das Gravitationsfeld einer Kugel aus inkompressibler Flüssigkeit nach der Einsteinschen Theorie *Sitzungsberichte der Königlich Preussischen Akademie der Wissenschaften zu Berlin* pp 424–434 URL https://www.jp-petit.org/Schwarzschild-1916-interior-de.pdf

[78] Žofka M and Bičák J 2008 Cylindrical spacetimes with $\lambda \neq 0$ and their sources *Classical and Quantum Gravity* **25** 015011 URL https://doi.org/10.1088%2F0264-9381%2F25%2F1%2F015011

[79] Linet B 1986 The static, cylindrically symmetric strings in general relativity with cosmological constant *Journal of Mathematical Physics* **27** 1817–1818 URL https://doi.org/10.1063/1.527050

[80] Tian Q 1986 Cosmic strings with cosmological constant *Phys. Rev. D* **33**(12) 3549–3555 URL https://link.aps.org/doi/10.1103/PhysRevD.33.3549

[81] Lemos J P 1995 Three dimensional black holes and cylindrical general relativity *Physics Letters B* **353** 46–51 ISSN 0370-2693 URL http://www.sciencedirect.com/science/article/pii/037026939500533Q

[82] Övgün A 2019 Weak field deflection angle by regular black holes with cosmic strings using the Gauss-Bonnet theorem *Phys. Rev. D* **99**(10) 104075 URL https://link.aps.org/doi/10.1103/PhysRevD.99.104075

[83] Bronnikov K A, Bolokhov S V and Skvortsova M V 2019 Cylindrical wormholes: A search for viable phantom-free models in GR *International Journal of Modern Physics D* **28** 1941008 URL https://doi.org/10.1142/S0218271819410086

[84] Bolokhov S V, Bronnikov K A and Skvortsova M V 2019 Rotating cylinders with anisotropic fluids in general relativity *Gravitation and Cosmology* **25** 122–130 ISSN 1995-0721 URL https://doi.org/10.1134/S020228931902004X

[85] Griffiths J B and Santos N O 2010 A rotating cylinder in an asymptotically locally anti-de Sitter background *Classical and Quantum Gravity* **27** 125004 URL https://doi.org/10.1088%2F0264-9381%2F27%2F12%2F125004

[86] Bini D, Geralico A and Plastino W 2019 Cylindrical gravitational waves: C-energy, super-energy and associated dynamical effects *Classical and Quantum Gravity* **36** 095012 URL https://doi.org/10.1088%2F1361-6382%2Fab10ec

[87] Žofka M, Boyd S T P, Kenkre V M and Duncan R V 1996 Analytic calculation of temperature error in sidewall thermometry measurements near T_λ in ^{4}He thermal conductivity cells *APS March Meeting Abstracts* APS Meeting Abstracts p A18.07

6 Selected original papers

In the following pages, as an illustration of my work on some of the topics of interest to me, I present a selection of my papers concerning the areas covered in the previous text. In particular, I attach a paper on the generalized Bonnor–Melvin spacetime discussed in Chapter 1

- Veselý J and Žofka M 2019 Cosmological magnetic field: The boost-symmetric case. *Physical Review D* **100** 044059
  URL `https://link.aps.org/doi/10.1103/PhysRevD.100.044059`,

2 papers on the Majumdar–Papapetrou solutions from Chapter 2

- Ryzner J and Žofka M 2015 Electrogeodesics in the di-hole Majumdar–Papapetrou spacetime. *Classical and Quantum Gravity* **32** 205010
  URL `https://doi.org/10.1088%2F0264-9381%2F32%2F20%2F205010`,

- Ryzner J and Žofka M 2016 Extremally charged line. *Classical and Quantum Gravity* **33** 245005
  URL `https://doi.org/10.1088%2F0264-9381%2F33%2F24%2F245005`,

a paper on the motion of extended bodies—the topic of Chapter 3

- Veselý V and Žofka M 2019 How to glide in Schwarzschild spacetime. *Classical and Quantum Gravity* **36** 075011
  URL `https://doi.org/10.1088%2F1361-6382%2Fab0976`,

2 papers on higher-dimensional extensions of Einstein gravity summarized in Chapter 4

- Ortaggio M, Podolský J and Žofka M 2008 Robinson–Trautman spacetimes with an electromagnetic field in higher dimensions. *Classical and Quantum Gravity* **25** 025006
  URL `https://doi.org/10.1088%2F0264-9381%2F25%2F2%2F025006`,

- Ortaggio M, Podolský J and Žofka M 2015 Static and radiating p-form black holes in the higher dimensional Robinson–Trautman class. *Journal of High Energy Physics* **2015** 45
  URL `https://doi.org/10.1007/JHEP02(2015)045`,

and 2 papers on other cylindrically symmetric spacetimes discussed in Chapter 5

- Bičák J, Ledvinka T, Schmidt B G and Žofka M 2004 Static fluid cylinders and their fields: global solutions. *Classical and Quantum Gravity* **21** 1583-1608
  URL `https://doi.org/10.1088%2F0264-9381%2F21%2F6%2F019`,

- Žofka M and Bičák J 2008 Cylindrical spacetimes with $\Lambda \neq 0$ and their sources. *Classical and Quantum Gravity* **25** 015011
  URL `https://doi.org/10.1088%2F0264-9381%2F25%2F1%2F015011`.